

General Disclaimer

One or more of the Following Statements may affect this Document

- This document has been reproduced from the best copy furnished by the organizational source. It is being released in the interest of making available as much information as possible.
- This document may contain data, which exceeds the sheet parameters. It was furnished in this condition by the organizational source and is the best copy available.
- This document may contain tone-on-tone or color graphs, charts and/or pictures, which have been reproduced in black and white.
- This document is paginated as submitted by the original source.
- Portions of this document are not fully legible due to the historical nature of some of the material. However, it is the best reproduction available from the original submission.

(NASA-CR-150248) DIGITAL CONTINUOUS DESIGN:
CONTINUOUS AND DISCRETE DESCRIBING FUNCTION
ANALYSIS OF THE IFS SYSTEM Bimonthly Report
(Systems Research Lab., Champaign, Ill.)
56 P EC AC4/PI AC1

N77-22834

Unclas

CSCI CSE G3/60 26062

RESEARCH STUDY ON STABILIZATION AND CONTROL
MODERN SAMPLED-DATA CONTROL THEORY

SYSTEMS RESEARCH LABORATORY

P.O. BOX 2277, STATION A
3206 VALLEY BROOK DRIVE
CHAMPAIGN, ILLINOIS 61820

PREPARED FOR GEORGE C. MARSHALL SPACE FLIGHT CENTER
HUNTSVILLE, ALABAMA



BIMONTHLY REPORT

DIGITAL CONTROLLER DESIGN

subtitle:

CONTINUOUS AND DISCRETE
DESCRIBING FUNCTION ANALYSIS
OF THE IPS SYSTEM

April 1, 1977

Contract No. NAS8-32358 1-7-ED-07418(1F)

PREPARED FOR GEORGE C. MARSHALL SPACE FLIGHT CENTER

HUNTSVILLE, ALABAMA

SYSTEMS RESEARCH LABORATORY

P.O. BOX 2277, STATION A
CHAMPAIGN, ILLINOIS 61820

1

I. MODEL DEVELOPMENT OF THE CONTINUOUS-DATA IPS CONTROL SYSTEMS

The objective of this chapter is to develop the dynamic equations and the mathematical model of the continuous-data IPS control system. The IPS model considered includes one flexible body mode and is hardmounted to the Orbiter/Pallet. The model contains equations describing a torque feed-forward loop (using accelerometers as inputs) which will aid in reducing the pointing errors caused by Orbiter disturbances.

The equations of motion of the IPS system are written as

$$M\ddot{R} + D\dot{R} + KR + Q\int R dt = F \quad (1-1)$$

where

$$R = \begin{bmatrix} X_s \\ Z_s \\ \theta_s \\ \theta_i \\ X \\ Z \\ \eta \end{bmatrix} \quad (1-2)$$

X_s, Z_s : translations of the Orbiter

θ_s : attitude of the Orbiter

θ_i : attitude of the instrument

X, Z : accelerometer measurements

M : 7×7 mass matrix

D : 7×7 damping matrix

K : 7×7 stiffness matrix

Q : 7×7 integral control matrix

F : 7×1 generalized force vector

The elements of M are:

$$m_{11} = m_0 + m_i = 91,200$$

$$m_{13} = m_i (d_{sm} + c)_z = -226$$

$$m_{14} = m_i (m_{bz} c \phi + r_{bx} S \phi) = 2,270$$

$$m_{22} = m_0 + m_i = 91,200$$

$$m_{23} = -m_i (d_{sm} + c)_x = 16,600$$

$$m_{24} = -m_i (-r_{bz} S \phi + r_{bx} C \phi) = 3,920$$

$$m_{31} = m_{13} = m_i (d_{sm} + c)_z = -226$$

$$m_{32} = m_{23} = 16,600$$

$$m_{33} = I_{0y} + I_{iy} + m_i ((d_{sm} + c)_x^2 + (d_{sm} + c)_z^2) = 7.06 \times 10^6$$

$$m_{34} = I_{iy} + m_i ((d_{sm} + c)_z (r_{bz} c \phi + r_{bx} S \phi) + (d_{sm} + c)_x (-r_{bz} S \phi + r_{bx} C \phi)) \\ = 26,700$$

$$m_{41} = m_{14} = 2,270$$

$$m_{42} = m_{24} = 3,920$$

$$m_{43} = m_{34} = 26,700$$

$$m_{44} = I_{iy} + m_i (r_{bx}^2 + r_{bz}^2) = 10,300$$

$$m_{51} = -1.0$$

$$m_{53} = -d_{smz} = 0.929$$

$$m_{55} = 1.0$$

$$m_{57} = h_x = -0.00113$$

$$m_{63} = d_{smx} = -4.72$$

$$m_{66} = 1.0$$

$$m_{67} = h_z = 0.00137$$

$$m_{77} = 1.0$$

$$m_{62} = -1$$

All other elements of M are zero.

The elements of D are:

$$d_{43} = d_{44} = K_r = 19,700$$

$$d_{47} = K_r \sigma_{rg} = -76.4$$

$$d_{55} = 2\zeta_x \omega_x = 44$$

$$d_{66} = 2\zeta_z \omega_z = 44$$

$$d_{77} = 2\zeta_b \omega_b = 0.115$$

All other elements of D are zero.

The elements of K are:

$$k_{43} = k_{44} = K_p = 70,000$$

$$k_{45} = -m_i (r_{bz} c\phi + r_{bx} s\phi) \omega_{ay}^2 = -2.23 \times 10^6$$

$$k_{46} = m_i (-r_{bz} s\phi + r_{bx} c\phi) \omega_{ay}^2 = -3.87 \times 10^6$$

$$k_{47} = K_p \sigma_{ss} = -272$$

$$k_{55} = \omega_x^2 = 986$$

$$k_{66} = \omega_z^2 = 986$$

$$k_{77} = \omega_b^2 = 132$$

All other elements of K are zero.

The elements of Q are:

$$q_{43} = q_{44} = K_i = 1.1 \times 10^5$$

$$q_{47} = K_i \sigma_{ss} = -427$$

All other elements of Q are zero.

The generalized force vector is

$$F = [F_x \quad F_z \quad r_{cx} F_z - r_{cz} F_x \quad 0 \quad 0 \quad 0 \quad h_{zc} F_z + h_{xc} F_x]' \quad (1-3)$$

Given the elements of the matrices M, D, K and Q, the equations of motion of Eq. (1-1) are written as

$$m_{11}\ddot{X}_s + m_{13}\ddot{\theta}_s + m_{14}\ddot{\theta}_i = F_x \quad (1-4)$$

$$m_{22}\ddot{Z}_s + m_{23}\ddot{\theta}_s + m_{24}\ddot{\theta}_i = F_z \quad (1-5)$$

$$m_{31}\ddot{X}_s + m_{32}\ddot{Z}_s + m_{33}\ddot{\theta}_s + m_{34}\ddot{\theta}_i = r_{cx}F_z - r_{cz}F_x \quad (1-6)$$

$$\begin{aligned} m_{41}\ddot{X}_s + m_{42}\ddot{Z}_s + m_{43}\ddot{\theta}_s + m_{44}\ddot{\theta}_i + K_r\dot{\theta}_s + K_r\dot{\theta}_i + K_r\sigma_{rg}\dot{\eta} \\ + K_p\theta_s + K_p\theta_i + k_{45}\dot{X} + k_{46}\dot{Z} + k_{47}\eta + K_i\int\theta_s dt \\ + K_i\int\theta_i dt + K_i\sigma_{ss}\int\eta dt = 0 \end{aligned} \quad (1-7)$$

$$m_{51}\ddot{X}_s + m_{53}\ddot{\theta}_s + m_{55}\ddot{X} + m_{57}\ddot{\eta} + d_{55}\dot{X} + k_{55}X = 0 \quad (1-8)$$

$$m_{62}\ddot{Z}_s + m_{63}\ddot{\theta}_s + m_{66}\ddot{Z} + m_{67}\ddot{\eta} + d_{66}\dot{Z} + k_{66}Z = 0 \quad (1-9)$$

$$m_{77}\ddot{\eta} + d_{77}\dot{\eta} + k_{77}\eta = h_{zc}F_z + h_{xc}F_x \quad (1-10)$$

Without the nonlinear wire-cable and flex-pivot torques, the control torque is expressed as

$$\begin{aligned} T_c = -K_r\dot{\theta}_s - K_r\dot{\theta}_i - K_p\theta_s - K_p\theta_i - K_i\int\theta_s dt - K_i\int\theta_i dt \\ - k_{45}\dot{X} - k_{46}\dot{Z} \end{aligned} \quad (1-11)$$

where K_r , K_p , and K_i are the rate, position, and integral constants of the controller, respectively.

The nonlinear torque due to the flex pivot and wire cable can be lumped into one operator N which operates on θ_i . Thus, the component, $-N(\theta_i)$, should be added to Eq. (1-11); i.e.,

$$\begin{aligned} T_c = -K_r\dot{\theta}_s - K_r\dot{\theta}_i - K_p\theta_s - K_p\theta_i - K_i\int\theta_s dt - K_i\int\theta_i dt \\ - k_{45}\dot{X} - k_{46}\dot{Z} - N(\theta_i) \end{aligned} \quad (1-12)$$

Solving for X_s from Eq. (1-4), we have

$$\ddot{X}_s = -\frac{m_{13}}{m_{11}}\ddot{\theta}_s - \frac{m_{14}}{m_{11}}\ddot{\theta}_i + \frac{1}{m_{11}}F_x \quad (1-13)$$

Solving for \ddot{Z}_s from Eq. (1-5), we have

$$\ddot{Z}_s = -\frac{m_{23}}{m_{22}} \ddot{\theta}_s - \frac{m_{24}}{m_{22}} \ddot{\theta}_i + F_z \frac{1}{m_{22}} \quad (1-14)$$

Substitute Eq. (1-13) and (1-14) into Eq. (1-6), we have

$$\begin{aligned} & -\frac{m_{31}m_{13}}{m_{11}} \ddot{\theta}_s - \frac{m_{31}m_{14}}{m_{11}} \ddot{\theta}_i + \frac{m_{31}}{m_{11}} F_x - \frac{m_{32}m_{23}}{m_{22}} \ddot{\theta}_s - \frac{m_{32}m_{24}}{m_{22}} \ddot{\theta}_i + \frac{m_{32}}{m_{22}} F_z \\ & + m_{33} \ddot{\theta}_s + m_{34} \ddot{\theta}_i = r_{cx} F_z - r_{cz} F_x \end{aligned} \quad (1-15)$$

The last equation is rearranged to the following form:

$$\begin{aligned} & \left(m_{33} - \frac{m_{31}m_{13}}{m_{11}} - \frac{m_{32}m_{23}}{m_{22}} \right) \ddot{\theta}_s + \left(m_{34} - \frac{m_{31}m_{14}}{m_{11}} - \frac{m_{32}m_{24}}{m_{22}} \right) \ddot{\theta}_i \\ & = r_{cx} F_z - r_{cz} F_x - \frac{m_{31}}{m_{11}} F_x - \frac{m_{32}}{m_{22}} F_z \end{aligned} \quad (1-16)$$

Substitute Eqs. (1-13) and (1-14) into Eq. (1-7), and making use of Eq. (1-12), we have

$$\begin{aligned} & m_{41} \left(-\frac{m_{13}}{m_{11}} \ddot{\theta}_s - \frac{m_{14}}{m_{11}} \ddot{\theta}_i + \frac{1}{m_{11}} F_x \right) + m_{42} \left(-\frac{m_{23}}{m_{22}} \ddot{\theta}_s - \frac{m_{24}}{m_{22}} \ddot{\theta}_i + F_z \frac{1}{m_{22}} \right) \\ & + m_{43} \ddot{\theta}_s + m_{44} \ddot{\theta}_i + K_{r\sigma rg} \dot{\eta} + k_{47} \eta + K_{i\sigma ss} \int \eta dt - T_c = 0 \end{aligned} \quad (1-17)$$

Simplifying, the last equation becomes

$$\begin{aligned} & \left(m_{43} - \frac{m_{13}m_{41}}{m_{11}} - \frac{m_{42}m_{23}}{m_{22}} \right) \ddot{\theta}_s + \left(m_{44} - \frac{m_{14}m_{41}}{m_{11}} - \frac{m_{42}m_{24}}{m_{22}} \right) \ddot{\theta}_i \\ & + K_{r\sigma rg} \dot{\eta} + k_{47} \eta + K_{i\sigma ss} \int \eta dt - T_c = -\frac{m_{41}}{m_{11}} F_x - \frac{m_{42}}{m_{22}} F_z \end{aligned} \quad (1-18)$$

Similarly, Eq. (1-9) is written as

$$m_{62} \left(-\frac{m_{23}}{m_{22}} \ddot{\theta}_s - \frac{m_{24}}{m_{22}} \ddot{\theta}_i + \frac{1}{m_{22}} F_z \right) + m_{63} \ddot{\theta}_s + m_{66} \ddot{Z} + m_{67} \ddot{\eta} + d_{66} \dot{Z} + k_{66} Z = 0 \quad (1-19)$$

Equations (1-16), (1-18), (1-19), (1-8) and (1-10) are now written as

$$M_s \ddot{\theta}_s + M_i \ddot{\theta}_i = - \left(r_{cz} + \frac{m_{31}}{m_{11}} \right) F_x + \left(r_{cx} - \frac{m_{32}}{m_{22}} \right) F_z \quad (1-20)$$

$$M_k \ddot{\theta}_s + M_n \ddot{\theta}_i + K_{r\sigma} \dot{\eta} + k_{47} \eta + K_{i\sigma} \int \eta dt - T_c = - \frac{m_{41}}{m_{11}} F_x - \frac{m_{42}}{m_{22}} F_z \quad (1-21)$$

where

$$M_s = m_{33} - \frac{m_{13}m_{31}}{m_{11}} - \frac{m_{32}m_{23}}{m_{22}} \quad (1-22)$$

$$M_i = m_{34} - \frac{m_{31}m_{14}}{m_{11}} - \frac{m_{32}m_{24}}{m_{22}} \quad (1-23)$$

$$M_k = m_{43} - \frac{m_{13}m_{41}}{m_{11}} - \frac{m_{42}m_{23}}{m_{22}} \quad (1-24)$$

$$M_n = m_{44} - \frac{m_{14}m_{41}}{m_{11}} - \frac{m_{42}m_{24}}{m_{22}} \quad (1-25)$$

$$M_p \ddot{\theta}_s + M_r \ddot{\theta}_i + m_{66} \ddot{z} + m_{67} \ddot{\eta} + d_{66} \dot{z} + k_{66} z = - \frac{m_{62}}{m_{22}} F_z \quad (1-26)$$

where

$$M_p = - \frac{m_{62}m_{23}}{m_{22}} + m_{63} \quad (1-27)$$

$$M_r = - \frac{m_{62}m_{24}}{m_{22}} \quad (1-28)$$

$$M_u = M_{53} - \frac{m_{51}m_{13}}{m_{11}} \quad (1-29)$$

$$M_v = - \frac{m_{51}m_{14}}{m_{11}} \quad (1-30)$$

$$\left(m_{53} - \frac{m_{51}m_{13}}{m_{11}} \right) \ddot{\theta}_s - \frac{m_{51}m_{14}}{m_{11}} \ddot{\theta}_i + m_{55} \ddot{x} + m_{57} \ddot{\eta} + d_{55} \dot{x} + k_{55} x = - \frac{m_{51}}{m_{11}} F_x \quad (1-31)$$

$$m_{77} \ddot{\eta} + d_{77} \dot{\eta} + k_{77} \eta = h_{zc} F_z + h_{xc} F_x \quad (1-32)$$

These last five differential equations are rearranged so that a block diagram

can be constructed.

$$\ddot{\theta}_s = -\frac{M_i}{M_s} \ddot{\theta}_i - \frac{1}{M_s} \left(r_{cz} + \frac{m_{31}}{m_{11}} \right) F_x + \frac{1}{M_s} \left(r_{cx} - \frac{m_{32}}{m_{22}} \right) F_z \quad (1-33)$$

$$\begin{aligned} \ddot{\theta}_i = & -\frac{M_k}{M_n} \ddot{\theta}_s - \frac{K_r \sigma_{rg}}{M_n} \dot{\eta} - \frac{k_{47}}{M_n} \eta - \frac{K_i \sigma_{ss}}{M_n} \int \eta dt + \frac{1}{M_n} T_c \\ & - \frac{m_{41}}{M_n m_{11}} F_x - \frac{m_{42}}{M_n m_{11}} F_z \end{aligned} \quad (1-34)$$

$$\ddot{z} = -\frac{M_p}{m_{66}} \ddot{\theta}_s - \frac{M_r}{m_{66}} \ddot{\theta}_i - \frac{m_{67}}{m_{66}} \ddot{\eta} - \frac{d_{66}}{m_{66}} \dot{z} - \frac{k_{66}}{m_{66}} z - \frac{m_{62}}{m_{22} m_{66}} F_z \quad (1-35)$$

$$\ddot{x} = -\frac{M_u}{m_{55}} \ddot{\theta}_s - \frac{M_v}{m_{55}} \ddot{\theta}_i - \frac{m_{57}}{m_{55}} \ddot{\eta} - \frac{d_{55}}{m_{55}} \dot{x} - \frac{k_{55}}{m_{55}} x - \frac{m_{51}}{m_{11} m_{55}} F_x \quad (1-36)$$

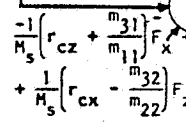
$$\ddot{\eta} = -\frac{d_{77}}{m_{77}} \dot{\eta} + \frac{k_{77}}{m_{77}} \eta + \frac{h_{zc}}{m_{77}} F_z + \frac{h_{xc}}{m_{77}} F_x \quad (1-37)$$

The control torque T_c is given by Eq. (1-12).

The block diagram which portrays the differential equations of Eqs. (1-33) through (1-37) is shown in Fig. 1-1. The nonlinear element which represents the nonlinear torque due to the flex pivot and wire cable is also included in the block diagram. The signal flow graph representation of Fig. 1-1 for the purpose of evaluating the determinant is shown in Fig. 1-2. The dynamics of η is eliminated since they do not enter the determinant of the signal flow graph.

Applying Mason's gain formula to Fig. 1-2, the determinant of the signal flow graph is evaluated as follows:

$$\Delta = 1 + \frac{Ns + K_p s + K_i + K_r s^2 - \frac{M_v}{m_{55}} k_{45} G_x s^3 - \frac{M_r}{m_{66}} k_{46} G_z s^3}{M_n s^3}$$



CO
:-)

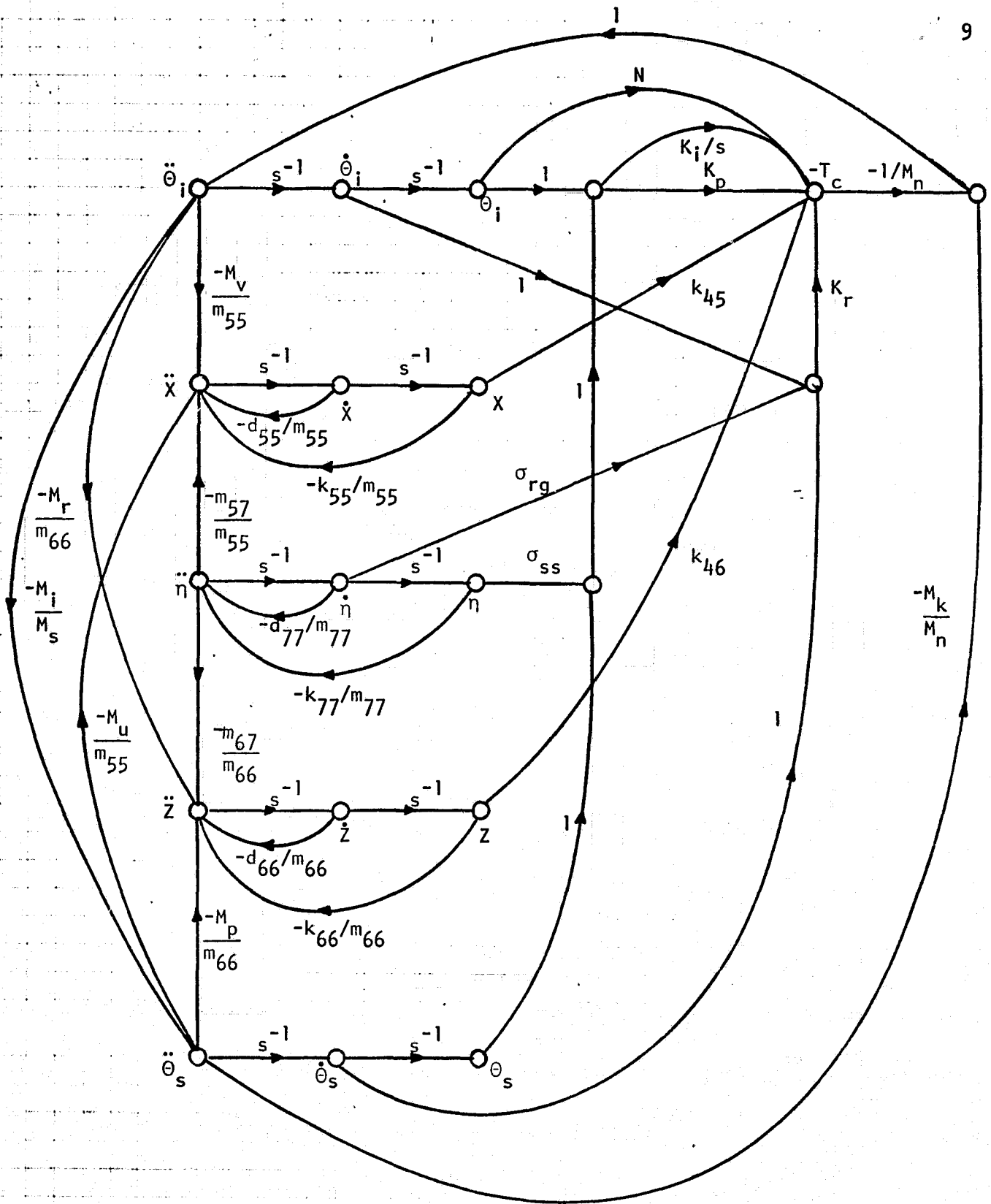


Figure 1-2. Signal flow graph of the IPS system.

$$+ \frac{M_i \left(\frac{M_u}{m_{55}} k_{45} G_x s^3 + \frac{M_p k_{46}}{m_{66}} G_z s^3 - K_p s - K_i - K_r s^2 - M_k s^3 \right)}{M_s M_n s^3} = 0 \quad (1-38)$$

where

$$G_x = \frac{1}{s^2 + \frac{d_{55}}{m_{55}} s + \frac{k_{55}}{m_{55}}} \quad (1-39)$$

$$G_z = \frac{1}{s^2 + \frac{d_{66}}{m_{66}} s + \frac{k_{66}}{m_{66}}} \quad (1-40)$$

Rearranging both sides of Eq. (1-38), we have

$$\begin{aligned} & M_s M_n s^3 + M_s \left(N s + K_p s + K_i + K_r s^2 - \frac{M_v}{m_{55}} k_{45} G_x s^3 - \frac{M_r}{m_{66}} k_{46} G_z s^3 \right) \\ & + M_i \left(\frac{M_u}{m_{55}} k_{45} G_x s^3 + \frac{M_p k_{46}}{m_{66}} G_z s^3 - K_p s - K_i - K_r s^2 - M_k s^3 \right) = 0 \end{aligned} \quad (1-41)$$

Dividing both sides of the last equation by the terms that do not contain N , we get the equivalent linear transfer function that the nonlinear element N sees,

$$\begin{aligned} G_{eq}(s) &= \frac{M_s s}{(M_s M_n - M_i M_k) s^3 + M_s \left(K_p s + K_i + K_r s^2 - \frac{M_v}{m_{55}} k_{45} G_x s^3 - \frac{M_r}{m_{66}} k_{46} G_z s^3 \right)} \\ &+ M_i \left(\frac{M_u}{m_{55}} k_{45} G_x s^3 + \frac{M_p k_{46}}{m_{66}} G_z s^3 - K_p s - K_i - K_r s^2 \right) \end{aligned} \quad (1-42)$$

For the system parameters given, $G_x = G_z$; thus, Eq. (1-42) is simplified to

$$\begin{aligned} G_{eq}(s) &= \frac{M_s s \left(s^2 + \frac{d_{55}}{m_{55}} s + \frac{k_{55}}{m_{55}} \right)}{\left((M_s M_n - M_i M_k) s^3 + (M_s - M_i) (K_r s^2 + K_p s + K_i) \right) \left(s^2 + \frac{d_{55}}{m_{55}} s + \frac{k_{55}}{m_{55}} \right)} \\ &+ \left(\frac{M_i M_u - M_s M_v}{m_{55}} \right) k_{45} s^3 + \left(\frac{M_i M_p - M_s M_r}{m_{66}} \right) k_{46} s^3 \end{aligned} \quad (1-43)$$

Substitution of the system parameters into Eq. (1-43) with

$$M_s = 7056977.95$$

$$M_k = M_i = 25992.12$$

$$M_n = 10074.90$$

$$M_u = 0.926522$$

$$M_p = -4.537982$$

$$M_r = 0.042982$$

$$M_v = 0.02489$$

we have

$$G_{eq}(s) = \frac{1.002077 \times 10^{-4} s(s^2 + 44s + 986)}{s^5 + 45.96676s^4 + 1107.4783s^3 + 2257.769s^2 + 7374.0808s + 10828.48765} \quad (1-44)$$

It is interesting to note that the system shown in Fig. 1-1 is of the 11th order. However, since the dynamics of η do not enter the picture on the stability of the nonlinear system, and since $G_x = G_z$, the transfer function seen by N is only of the 5th order.

II. PREDICTION OF SELF-SUSTAINED OSCILLATIONS OF THE CONTINUOUS-DATA IPS SYSTEM WITH WIRE-CABLE AND FLEX-PIVOT NONLINEARITIES

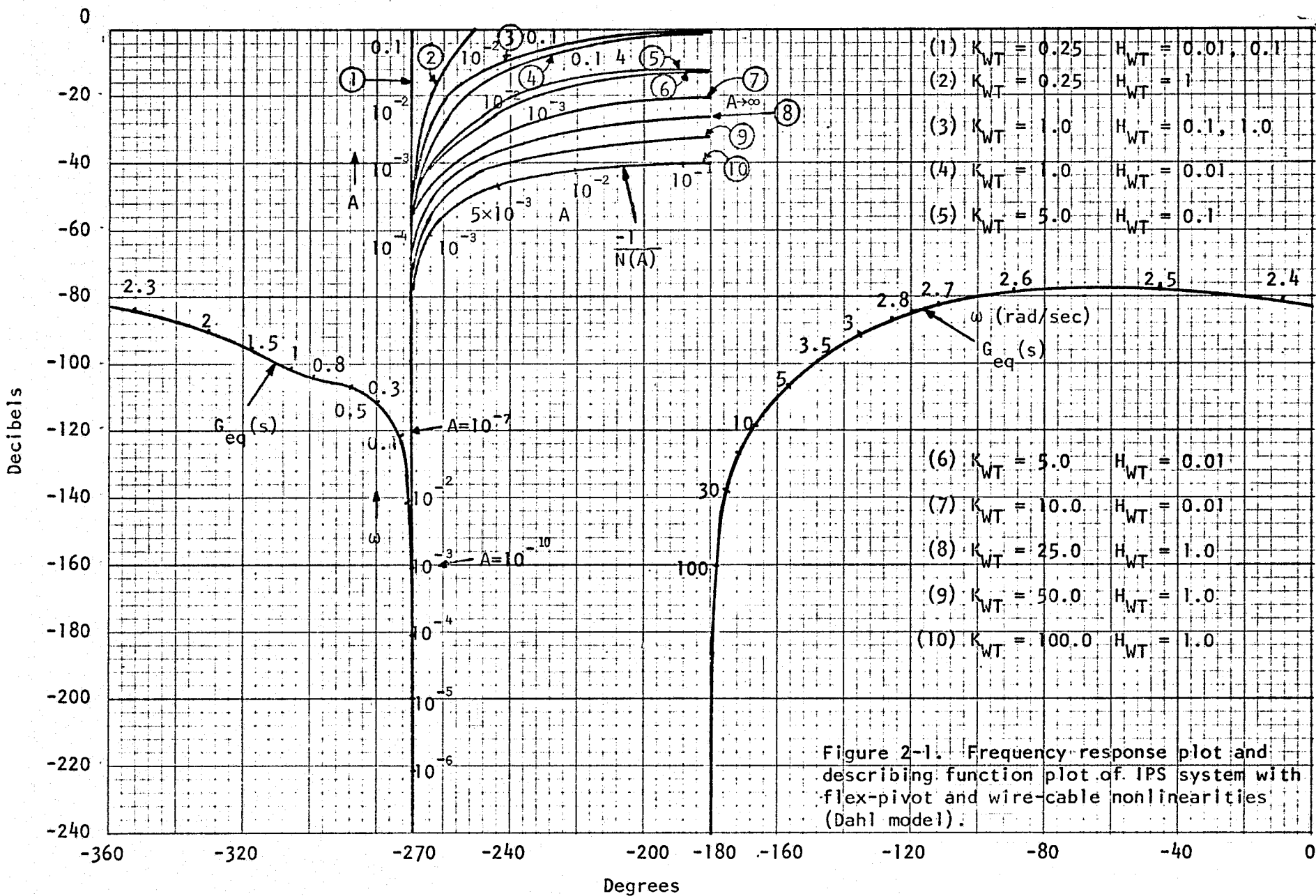
The equivalent transfer function $G_{eq}(s)$ in Eq. (1-44) can be plotted in the gain-phase coordinates together with the plot of $-1/N$ of the nonlinear element for stability analysis. The describing function of the combined flex-pivot and wire-cable nonlinearity using the Dahl model has been derived in [1]. In this earlier report a simplified model of the IPS system was obtained by assuming that all but motion about two of the seven degrees of freedom of axes are negligible. Only motion about the scientific instrument axis and the mount rotation were considered.

For the purpose of comparison, the equivalent transfer function that the nonlinearity sees for the simplified IPS in [1] is repeated as follows:

$$G_{eq}(s) = \frac{0.0013946s(s^2 + 0.0012528s + 0.0036846)}{s^5 + 16.7s^4 + 222.6s^3 + 279.806s^2 + 5.857s + 5.13855} \quad (2-1)$$

when the integral control constant K_I is 10^6 . The zeros of this transfer function are $s = -0.0006264 + j0.06069764$ and $s = -0.0006264 - j0.06069764$. The five poles are at $s = -1.38135$, $s = -0.0031956 + j0.135895$, $s = -0.0031956 - j0.135895$, $s = -7.65618 + j11.946$, and $s = -7.65618 - j11.946$. It was concluded in [1] from the gain-phase plot of $G_{eq}(s)$ versus the $-1/N(A)$ plot that the simplified IPS may have a sustained oscillation that is characterized by the frequency of $\omega = 0.16$ rad/sec. Depending on the values of the parameters of the wire-cable and flex-pivot nonlinearities, K_{WT} and H_{WT} , the amplitude of oscillation of ϵ , which is comparable to θ_i in this report, lies between 3×10^{-8} to 3×10^{-6} for $K_I = 10^6$.

The equivalent transfer function of Eq. (1-44) is plotted as shown in Fig. 2-1. It is noted that the IPS model used in the present work does not



have the same system parameters as the simplified IPS system studied in [1]. Thus, the natural frequencies of the two systems are different. From Fig. 2-1 it is observed that the $G_{eq}(s)$ and $-1/N$ loci would intersect only at very low frequencies and when the amplitude of oscillation is extremely small. For instance, at $\omega = 10^{-3}$ rad/sec, the amplitude of oscillation is approximately 10^{-10} , and for all practical purposes this can be regarded as zero. Thus, the IPS model considered here would not exhibit sustained oscillations due to the wire-cable and flex-pivot nonlinearities.

It is of interest to investigate the poles and zeros of the transfer function of Eq. (1-44). The poles and zeros of $G_{eq}(s)$ of Eq. (1-44) are tabulated as follows:

zeros: $s = 0, \quad -22 + j22.4053565, \quad -22 - j22.4053565$

poles: $s = -1.66963, \quad -0.123519 + j2.5232$

$-0.123519 - j2.5232$

$-22.025 + j23.0467$

$-22.025 - j23.0467$

The natural frequency of the dominant poles of the $G_{eq}(s)$ of Eq. (1-44) is found to be at 2.5232 rad/sec. This is much higher than that of the transfer function of Eq. (2-1). Furthermore, the two zeros listed above are very close to two of the poles.

III. DIGITAL COMPUTER SIMULATION OF THE CONTINUOUS-DATA NONLINEAR IPS CONTROL SYSTEM WITH DAHL MODEL AND ONE FLEXIBLE BODY MODE

The IPS control system with one flexible body mode and the nonlinear flex pivot torque modelled by the Dahl solid friction model ($i = 2$) is simulated on the digital computer. A block diagram of the IPS system is shown in Fig. 1-1. For the Dahl model with $i = 2$, the following parameters are used:

$$\gamma = 9.2444 \times 10^4$$

$$T_{FPO} = 2.25 \times 10^{-3} \text{ N-M}$$

The objective of the computer simulation of the system is to verify and/or clarify the analysis results obtained by the describing function method in Chapter II. Although the describing function method analysis in Chapter II does not yield precise results for possible amplitudes and frequencies of sustained oscillations, it does indicate that for the sets of system parameters used if sustained oscillations were to exist the amplitude of oscillation would be approximately less than 10^{-9} radians and the frequencies would be less than 10^{-3} radians/sec.

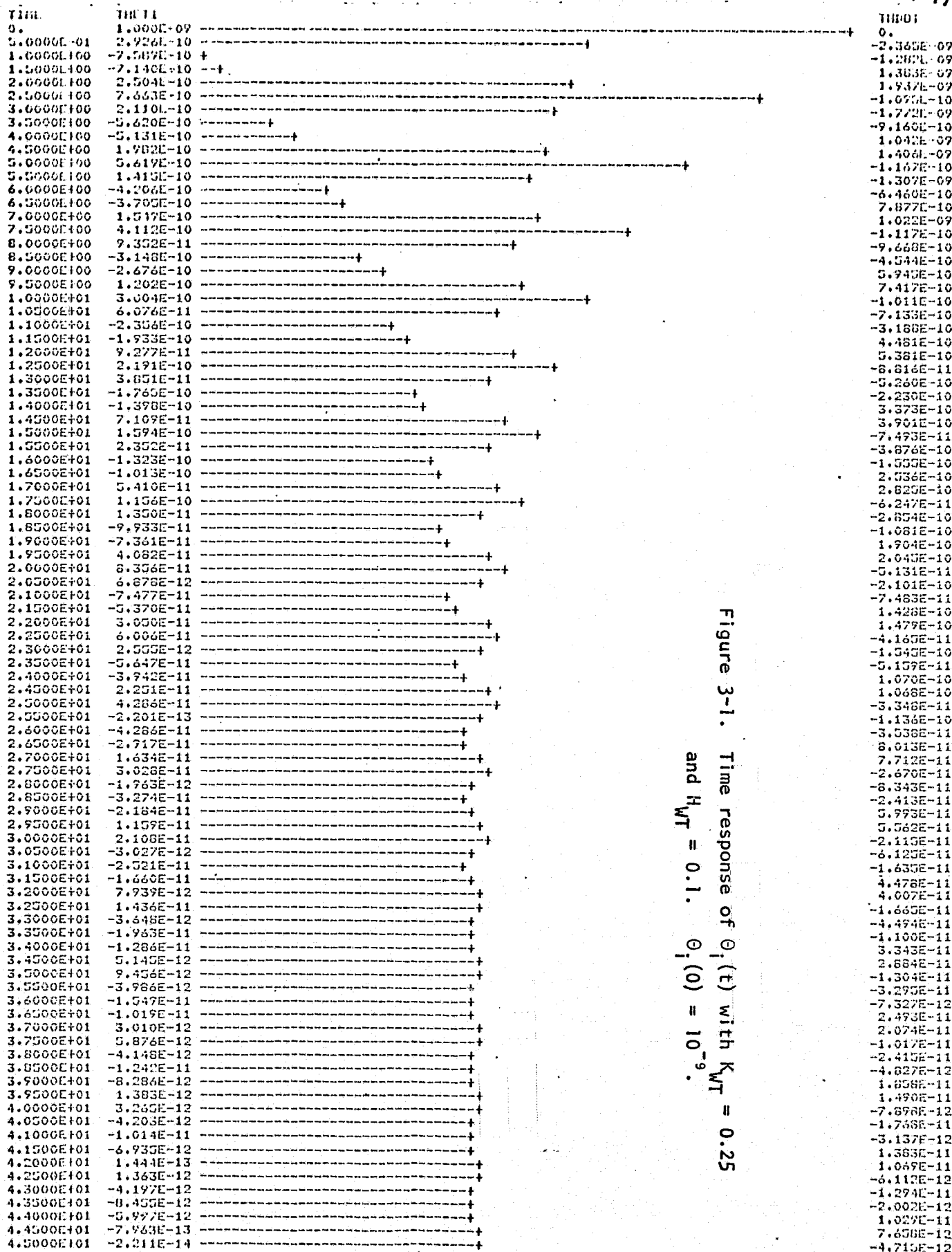
Since the significant time constant of the IPS system is very long, it would require a long computer simulation time to verify the existence or nonexistence of a limit cycle. Normally, the possibility of sustained oscillations could be checked by using two computer simulations, one with initial conditions that correspond to above and the other with initial conditions that correspond to below the value of the predicted amplitude of oscillations. If a sustained oscillation exists then the simulation with initial conditions below the predicted amplitude will result in a response that oscillates near the predicted frequency and increases in

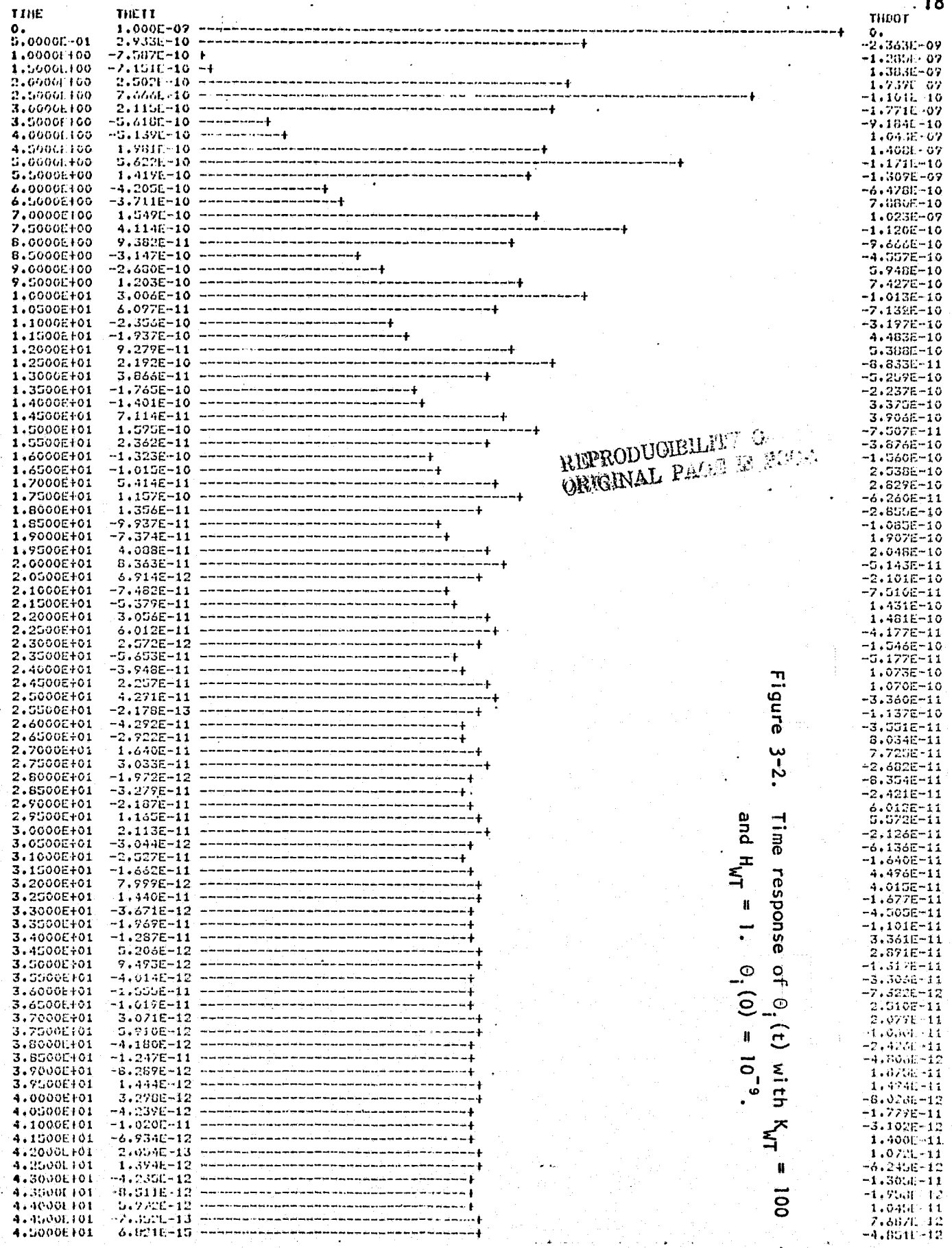
amplitude. Also, the simulation with initial conditions that correspond to an initial amplitude above the predicted amplitude will result in a response that decreases in amplitude and oscillates near the predicted frequency. However, since the analysis of Chapter II does not predict any specific sustained oscillations, the method described above must be changed.

Since the analysis of Chapter II provides no specific candidates for amplitudes and frequencies of limit cycles (or the amplitude and frequencies are all extremely small), it may be necessary to check for the absence of limit cycles. The absence of limit cycles can be verified by showing that the responses of the system due to any initial conditions actually decay to zero as time increases indefinitely.

Again, since the time constant of the IPS system is very long, the simulation of the system response by a digital computer may involve excessive computer time. Since if sustained oscillations were to exist, the possible frequencies of oscillations would be less than 10^{-3} rad/sec, the simulation time required would be in excess of $2\pi \times 10^3$ sec. Also, a double-precision program with 30 digits of accuracy would be required, since the amplitude of oscillation must be less than 10^{-9} radians. Instead, the results from the simulation will be used to verify that the oscillations of the system are damped out at a mode that is practically independent of the nonlinearity.

As a means of exciting the system, an initial perturbation of $\theta_i(0) = 10^{-9}$ radians was applied to the system. Two simulations of the system were completed for two extreme sets of wire cable parameters (K_{WT} and H_{WT}). The responses of θ_i for both of these cases are shown in Figs. 3-1 and 3-2. These responses indicate that the influence of the wire cable parameters on the system response is very insignificant. In addition, the frequency of





REPRODUCIBILITY 0.
ORIGINAL PAGE IS 2004.

Figure 3-2. Time response of $\theta_1(t)$ with $K_{WT} = 100$ and $H_{WT} = 1$. $\theta_1(0) = 10^{-9}$.

oscillation is approximately 2.5 rad/sec, which is approximately 10^4 times greater than the maximum possible frequency of oscillation. Also, the envelope of the response is decaying with a mode of $\sigma = -0.1239$, where $1/\sigma$ is considered as the time constant. Hence, the system over the 50 sec interval of simulation time has a response due to a pair of poles at $s = -0.1239 + j2.5$ and $s = -0.1239 - j2.5$, which is approximately one of the pairs of poles of $G_{eq}(s)$. Thus, the system oscillates at the dominant mode of $G_{eq}(s)$ as expected, if the system had no limit cycles and the nonlinearity were replaced by a unity gain element. This implies that the nonlinearity has very little influence on the the system response under the simulated conditions, and that no limit cycles exist.

Since the size of the feasible amplitudes predicted is so small, at least 15 digits are needed to carry out the 50 seconds of computer simulation.

The listing of the computer simulation program is given in Table 3-1.

```

PROGRAM IPSSIM(INPUT,IPSD2,TAPE6=IPSD2,OUTPUT=IPSD2)
IMPLICIT REAL(M)
COMMON SIGSS,AKI,AKP,AKR,AK45,AK46,SIGPG,D77,M77,AK77,HZC,HXC
1,MPT,MK,MS,MN,M41,M11,M31,RCZ,M42,RCY,M32,M22,D55
2,AK55,M51,M55,M57,MU,MV,D66,M66,MP,MR,AK66,M67,M62,
3,HWT,AKWT,RQ,SI,SLAST,TFP0,II
EXTERNAL PCTY,OUTP
DIMENSION Y(11),DERY(11),AUX(8,11),PRMT(7)
C NONLINEARITY CONSTANTS
AKWT=1.0E2$HWT=1.E0
GAMA=9.2444E4$TFP0=2.25E-3
G1=GAMA*TFP0
C INITIAL CONDITIONS
Y(3)=1.E-9$SLAST=Y(3)
II=0
A=2.E0*G1*SLAST
A1=1.E0/A
R0=-1.E0*(-A1+SQRT(A1**2+1.E0))
C INITIALIZE STATES
NDIM=11
DO 1 I=1,NDIM
IF(I.EQ.3) GO TO 1
Y(I)=0.E0
1 CONTINUE
C SET SYSTEM CONSTANTS
C MASS CONSTANTS ARE:
M11=9.12E4$M13=-2.26E2$M14=2.27E3
M22=M11$M23=1.56E4$M24=3.92E3
M31=M13$M32=123$M33=7.06E6$M34=2.67E4
M41=M14$M42=124$M43=M34$M44=1.03E4
M51=-1.E0$M53=9.29E-1$M55=1.E0$M57=-1.13E-3
M62=-1.E0$M63=-4.72E0$M66=M55$M67=1.37E-3
M77=M55
C SET DAMPING CONSTANTS
D43=1.97E4$D44=D43$D47=-76.4E0
D55=44.E0$D66=D55$D77=.115E0
C SET STIFFNESS CONSTANTS
AK43=7.E4$AK44=AK43$AK45=-2.23E6
AK46=-3.87E6$AK47=-2.72E2$AK55=9.86E2
AK66=9.35E2$AK77=1.32E2
C SET PID CONSTANTS
AKR=D44$SIGRG=D47/AKR
AKP=AK44$SIGSS=AK47/AKP
Q43=1.1E5$AKI=Q43$Q44=Q43
Q47=-4.27E2
C SET DISTANCES FROM CENTER OF MASSES & CENTER OF GRAVITIES
C SET TO ONE IF THE CREW MOTION IS NOT INCLUDED IN THE MODEL
HZC=1.E0$HXC=1.E0
RCY=1.E0$RCZ=1.E0
C DEFINE AGGREGATE MASS ELEMENTS
MI=M34-M31*M14/M11-M32*M24/M22
MK=M43-M13*M41/M11-M42*M23/M22
MS=M33-M13*M31/M11-M32*M23/M22
MN=M44-M14*M41/M11-M42*M24/M22
MU=M53-M51*M13/M11
MV=-M51*M14/M11
MP=-M52*M23/M22+M63
MR=-M52*M24/M22
C SET ERROR WEIGHTING FACTORS
DO 5 I=1,NDIM
DERY(I)=1.00/11.E0
5 CONTINUE
C SET RKGS CONTROL PARAMETERS
PRMT(1)=0.E0
PRMT(2)=0.5E2
PRMT(3)=1.E-2
PRMT(4)=1.E-14
PRMT(5)=0.E0
PRMT(6)=2.5E-1
PRMT(7)=PRMT(1)
CALL RKGS(PRMT,Y,DERY,NDIM,IHLE,PCTY,OUTP,AUX)
STOP
END

```

REPRODUCED FROM THE
ORIGINAL PAGE

Table 3-1 (continued).

```

SUBROUTINE OUTP (TIME, Y, DERY, IHLF, NDIM, PRMT)
DIMENSION Y (NDIM), DERY (NDIM), PRMT (7)
DEL=TIME-PRMT (7)
IF (ABS (TIME-PRMT (7)).LE.1.E-10) GO TO 1
IF (ABS (PRMT (5)-DEL).LE.1.E-10) GO TO 1
RETURN
1 PRMT (7)=TIME
WRITE (6,10) IHLF, TIME, Y (3), Y (8)
10 FORMAT (I6,1P2E10.4,1P2E11.3)
RETURN
END

```

```

SUBROUTINE FCTY (TIME, STATE, STDOT, KEEP, NDIM)
IMPLICIT REAL (M)
COMMON SIGSS, AKI, AKP, AKR, AK45, AK46, SIGRG, D77, M77, AK77, HZC
1, HXC, MI, MK, M5, MN, M41, M11, M31, PCZ, M42, RCY, M32, M22, D55
2, AK55, M51, M55, M57, MU, MV, D66, M66, MP, MR, AK66, M67, M62, HWT,
3 AKWT, R0, G1, SLAST, TFP0, II
C THIS SUBROUTINE ONLY UPDATES THE DERIVATIVE OF THE STATE VECTOR.
C THE UPDATE DEPENDS ON THE INPUTS, TIME, STATE, & KEEP.
DIMENSION STATE (NDIM), STDOT (NDIM)
FX (TIME)=0.E0
FZ (TIME)=0.E0
C 10 FORMAT (I6,1P2E10.4,1P2E11.3)
C MODEL THE WIRE NONLINEARITY
SGNEDT=1.E0
IF (STATE (3).LT.0.E0) SGNEDT=-1.E0
TWC=SGNEDT*HWT*AKWT*STATE (3)
C MODEL FOR THE DAHL NONLINEARITY (I=2)
IF ((TIME.GT.0.E0).AND.(KEEP.EQ.0)) GO TO 1
GO TO 2
1 II=1
2 R1=R0-SGNEDT
TFP=(SGNEDT+R1/(1.E0-G1*(STATE (3)-SLAST)*R1))*TFP0
IF (TFP.GT.TFP0) TFP=TFP0
IF (TFP.LT.-TFP0) TFP=-TFP0
IF (II.EQ.0) GO TO 3
R0=TFP/TFP0
II=0
SLAST=STATE (3)
GO TO 2
3 TFP=3.E0*TFP
ENN=TFP+TWC
STDOT (1)=STATE (5)
STDOT (2)=STATE (7)
STDOT (3)=STATE (3)
STDOT (4)=STATE (9)
STDOT (5)=STATE (10)
STDOT (11)=STATE (2)+STATE (3)+SIGSS*STATE (1)
PCM=ENN+AKI*STATE (11)+AKP*STDOT (11)+AK45*STATE (4)+AK46*STATE (
15)+AKR*(STATE (7)+STATE (8))+SIGRG*STATE (6))
STDOT (6)=-D77/M77*STATE (5)-AK77/M77*STATE (1)
1+HZC/D77*FZ (TIME)+FX (TIME)*HXC/D77
STDOT (7)=1.E0/(1.E0-MI*MK/M5/MN)*(MI/MS/MN*PCM+(MI*M41/(MS*MN*
1411)-(RCZ+M31/M11)/MS)*FX (TIME)+(MI*M42/(MS*MN*M11)+(PCZ
1-M32/M22)/MS)*FZ (TIME))
STDOT (8)=-1K/MN*STDOT (7)-TCM/MN-M41/MN/M11*FX (TIME)-M42/MN/
1M11*FZ (TIME)
STDOT (9)=-D55/M55*STATE (9)-AK55/M55*STATE (4)-M51/M11/M55*FX (
1 TIME)-M57/M55*STDOT (5)-MU/M55*STDOT (7)-MV/M55*STDOT (8)
STDOT (10)=-D66/M66*STATE (10)-AK66/M66*STATE (5)-M67/M66*STDOT (
15)-MP/M66*STDOT (7)-MR/M66*STDOT (8)-M62/M22/M66*FZ (TIME)
KEEP=1
RETURN
END

```

END OF INNERMOST RUNGE-KUTTA LOOP

```

CC 15 TEST OF ACCURACY
CC IF (ITEST) 16, 16, 20
CC
CC 16 IN CASE ITEST=0 THERE IS NO POSSIBILITY FOR TESTING OF ACCURACY
CC 17 DO 17 I=1, NDIM
CC 17 AUX(4, I) = Y(I)
CC ITEST=1
CC 18 ISTEP=ISTEP+ISTEP-2
CC 18 IHLF=IHLF+1
CC X=X-H
CC H=.5*H
CC DO 19 I=1, NDIM
CC Y(I)=AUX(1, I)
CC DERY(I)=AUX(2, I)
CC 19 AUX(5, I)=AUX(3, I)
CC GOTO 9
CC
CC 20 IN CASE ITEST=1 TESTING OF ACCURACY IS POSSIBLE
CC 20 IMOD=ISTEP/2
CC IF (ISTEP-IMOD-IMOD) 21, 23, 21
CC 21 CALL FCT(X, Y, DERY, KEEP, NDIM)
CC DO 22 I=1, NDIM
CC AUX(5, I) = Y(I)
CC 22 AUX(7, I) = DERY(I)
CC GOTO 9
CC
CC 23 COMPUTATION OF TEST VALUE DELT
CC 23 DELT=0.
CC DO 24 I=1, NDIM
CC 24 DELT=DELT+AUX(8, I)*ABS(AUX(4, I)-Y(I))
CC IF (DELT-PRMT(1+3)) 28, 29, 25
CC
CC 25 ERROR IS TOO GREAT
CC IF (IHLF-1) 26, 36, 36
CC 26 DO 27 I=1, NDIM
CC 27 AUX(4, I)=AUX(5, I)
CC ISTEP=ISTEP+ISTEP-4
CC X=X-H
CC IEND=0
CC GOTO 18
CC
CC 28 RESULT VALUES ARE GOOD
CC 28 KEEP=0
CC CALL FCT(X, Y, DERY, KEEP, NDIM)
CC DO 29 I=1, NDIM
CC AUX(1, I)=Y(I)
CC AUX(2, I)=DERY(I)
CC AUX(3, I)=AUX(6, I)
CC Y(I)=AUX(5, I)
CC 29 DERY(I)=AUX(7, I)
CC CALL OUTP(X, Y, DERY, IHLF, NDIM, PRMT)
CC IF (PRMT(1+4)) 40, 30, 45
CC 30 DO 31 I=1, NDIM
CC Y(I)=AUX(1, I)
CC 31 DERY(I)=AUX(2, I)
CC IREC=IHLF
CC IF (KEEP, 32, 2) GO TO 39
CC IF (IEND) 32, 32, 39
CC
CC 32 INCREMENT GETS DOUBLED
CC 32 IHLF=IHLF-1
CC ISTEP=ISTEP/2
CC H=H+H
CC IF (IHLF) 4, 33, 33
CC 33 IMOD=ISTEP/2
CC IF (ISTEP-IMOD-IMOD) 4, 34, 4
CC 34 IF (DELT-.02*PRMT(1+3)) 35, 35, 4
CC 35 IHLF=IHLF-1
CC ISTEP=ISTEP/2
CC H=H+H
CC GOTO 4

```

C
C

```

36 RETURNS TO CALLING PROGRAM
36 IHLF=11
  CALL FCT(X,Y,DERY,KEEP,NDIM)
  GOTO 39
37 IHLF=12
  GOTO 39
38 IHLF=13
39 CALL DUMP(X,Y,DERY,IHLF,NDIM,PRMT)
40 RETURN
  END

```

```

PROGRAM PLOTCE(INPUT,TAPE5=INPUT,GPH2,TAPF1=GPH2,IPSD2,
1 TAPE6=IPSD2)
  CALL GRAPH(1,"THETI",0.0,100.0,1,2,"THDOT",6,"DUMM1",1
1,"N",132)
  END

```

```

  SUBROUTINE GRAPH(NUMCOL,HEAD,FINIT,FINAL,NUMPRT,NUMP1,HEAD1,
  * NUMP2,HEAD2,NUMSKP,WAIT,NUMTTY)
  DIMENSION DATA(1000),TIMES(1000),CSTORE(81),DATA1(1000),
  * DATA2(1000),CARD(30),Y(15)

```

C *****

C THE GRAPHING PARAMETERS ARE THE FOLLOWING:

C NUMCOL= THE NO. OF THE COL. OF THE DATA FILE TO BE PLOTTED

C (AND PRINTED)

C HEAD = HEADING FOR THE PLOTTED VARIABLE (IN QUOTE MARKS)

C AINT = THE INITIAL PLOTTING TIME

C FINAL = THE FINAL PLOTTING TIME

C NUMPRT= THE NO. OF OTHER VARIABLES TO BE PRINTED ALONG SIDE

C THE GRAPH (1,1,2)

C NUMP1 = NO. OF THE COL. OF THE DATA FILE TO BE THE FIRST

C PRINTED VARIABLE

C HEAD1 = HEADING FOR THE FIRST PRINTED VARIABLE

C NUMP2 = NO. OF THE COL. OF THE DATA FILE TO BE THE SECOND

C HEAD2 = HEADING FOR THE SECOND PRINTED VARIABLE

C NUMSKP= NO. OF LINES OF DATA FILE TO BE SKIPPED BETWEEN

C SUCCESSIVE PRINTS (THIS ALLOWS THE GRAPH TO BE COMPRESSED)

C WAIT = "N" CAUSES THE PROG. TO WAIT FOR A CARRIAGE RETURN INPUT

C BEFORE IT STARTS TO PRINT. THIS ALLOWS TIME SO THE PAPER

C CAN BE POSITIONED TO THE TOP OF A NEW PAGE.

C NUMTTY= THE NO. OF CHARACTERS PER LINE OF TTY OUTPUT. (80,132)

C IF 80 IS USED THEN NO ADDITIONAL COLS. ARE PRINTED.

C INPUT FORMAT REQUIRED:

C FORMAT(6X,1PE10.4,1P10E11.3)

C 6X= THIS FIELD WIDTH CAN BE USED TO STORE IHLF OR SOME OTHER PARM.

C 1PE10.4= THIS FIELD IS USED TO STORE THE INDEPENDENT VARIABLE (TIME)

C 1P10E11.3= THESE FIELD WIDTHS CONTAIN UP TO 10 COLS. OF DATA

C FOR 10 DIFFERENT VARIABLES

C *****

```

  IF(WAIT.NE."N") GO TO 1001
  PRINT 1002
1002 FORMAT(" IS TTY SET FOR 132 (OR 80) CHARACTERS ?",/,
  * " TYPE CARRIAGE RETURN TO BEGIN OUTPUT")
  READ(5,1000) (CARD(L),L=1,80)
1000 FORMAT(80A1)
1001 ISKIP=30000
  TTYNUM=79.0
  IF(NUMTTY.EQ.132) GO TO 10
  TTYNUM=55.0
  NUMPRT=0
  ANAME="TIME "
  MAXNUM=0
  MAXCOL=NUMCOL
  IF(NUMP1.GT.MAXCOL) MAXCOL=NUMP1
  IF(NUMP2.GT.MAXCOL) MAXCOL=NUMP2
  READ(6,30) (TIME(X(L),L=1,MAXCOL)
  IF (EOF(6).NE.0) GO TO 100
30 FORMAT(6X,G10.4,10G11.3)

```

```

IF ((1.0E-05+TIME) .LT. AINIT) GO TO 20
ISKP=ISKP+1
IF (ISKP .LE. NUMSKP) GO TO 20
ISKP=0
IF ((TIME-1.0E-05) .GT. FINAL) GO TO 100
MAXNUM=MAXNUM+1
TIMES(MAXNUM)=TIME
DATA(MAXNUM)=X(NUMCOL)
DATA1(MAXNUM)=Y(NUMP1)
DATA2(MAXNUM)=X(NUMP2)
GO TO 20
100 IF (NUMPRT.EQ.0) WRITE(1,110) ANAME,HEAD
110 FORMAT(" ",A10,3X,A10)
120 IF (NUMPRT.EQ.1) WRITE(1,120) ANAME,HEAD,HEAD1
120 FORMAT(" ",A10,3X,A10,83X,A10)
130 IF (NUMPRT.EQ.2) WRITE(1,130) ANAME,HEAD,HEAD1,HEAD2
130 FORMAT(" ",A10,3X,A10,83X,A10,27,A10)
DMAX=DATA(1)
DMIN=DATA(1)
DO 50 M=2, MAXNUM
  DATAM=DATA(M)
  IF (DATAM.LT.DMAX) GO TO 40
  DMAX=DATAM
  IF (DATAM.GT.DMIN) GO TO 50
  DMIN=DATAM
50 CONTINUE
60 WIDTH=DMAX-DMIN
DO 80 M=1, MAXNUM
  K=1.0+((DATA(M)-DMIN)/WIDTH)*ETYNUM
  IF (K.EQ.1) GO TO 75
  IZ001=K-1
  DO 70 N=1, IZ001
    CSTORE(N)="-"
70 CSTORE(K)="+ "
75 IZ002=K+1
  DO 77 J=IZ002, 81
    CSTORE(J)="-"
77 IF (NUMPRT.EQ.0) WRITE(1,90) TIMES(M), DATA(M), (CSTORE(L), L=1, K)
90 FORMAT(" ",1PE10.4,1X,1PE11.3,1X,80A1)
  IF (NUMPRT.EQ.1) WRITE(1,92) TIMES(M), DATA(M), (CSTORE(L), L=1, 80),
  * DATA1(M)
  IF (NUMPRT.EQ.2) WRITE(1,92) TIMES(M), DATA(M), (CSTORE(L), L=1, 80),
  * DATA1(M), DATA2(M)
92 FORMAT(" ",1PE10.4,1X,1PE11.3,1X,80A1,1X,1PE11.3,1X,1PE11.3)
80 CONTINUE
RETURN
END

```

IV. DISCRETE DESCRIBING FUNCTION OF THE COMBINED WIRE-CABLE TORQUE AND FLEX-PIVOT NONLINEARITY

In the last three chapters the continuous-data IPS system with the combined nonlinearity of the wire-cable torque and flex pivot is studied. The describing function analysis is applied to the continuous-data system.

In the present chapter the digital IPS system with the combined nonlinearity is considered. The block diagram of the system is shown in Fig. 4-1. The combined nonlinearity is represented by the block N. The digital system is characterized by having the sample-and-hold units which have the notation S/H. In order to apply the discrete describing function technique, a sample-and-hold unit is inserted in the path of the nonlinearity N.

The objective of the investigation is to study whether self-sustained oscillations will occur in the digital IPS system. If self-sustained oscillations do occur, as they most likely will in a digital nonlinear system, what are the amplitudes and frequencies of these oscillations ?

4.1 Discrete Describing Function of the Combined Nonlinearity

The discrete model of the combined nonlinearity of the wire-cable torque and the flex-pivot characteristics is shown in Fig. 4-2. The zero-order hold at the input of the combined nonlinearity is deleted, since there is already a zero-order hold at the output of N.

The wire-cable torque T_{wc} is modelled as shown in Fig. 4-2 and is functionally represented by

$$T_{wc} = H_{WT} \text{SGN}(\dot{\theta}_i) + K_{WT} \theta_i \quad (4-1)$$

or

$$T_{wc}^+(\theta_i) = H_{WT} + K_{WT} \theta_i \quad \dot{\theta}_i \geq 0 \quad (4-2)$$

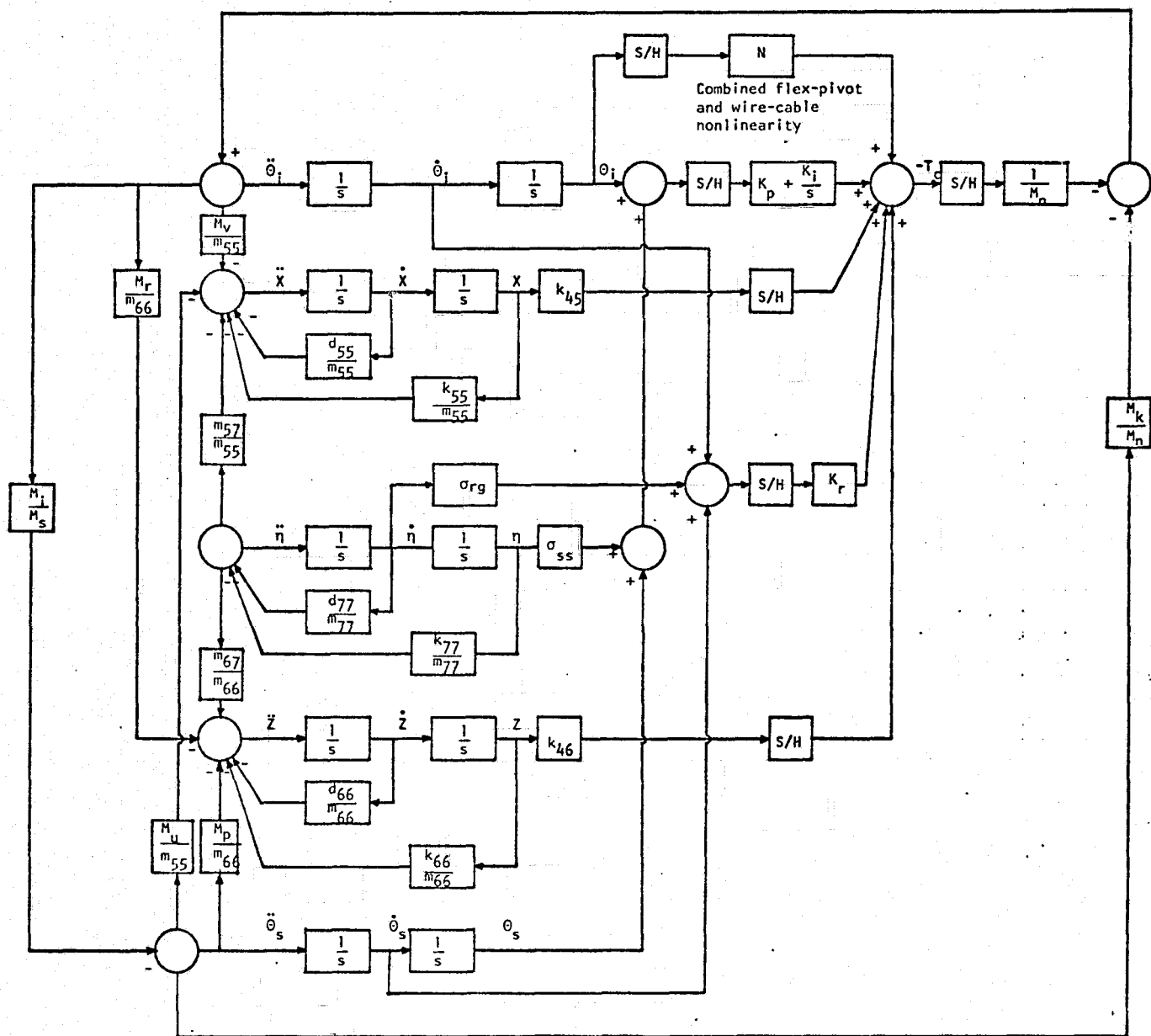


Figure 4-1. Block diagram of the digital IPS system with flex-pivot and wire-cable nonlinearities.

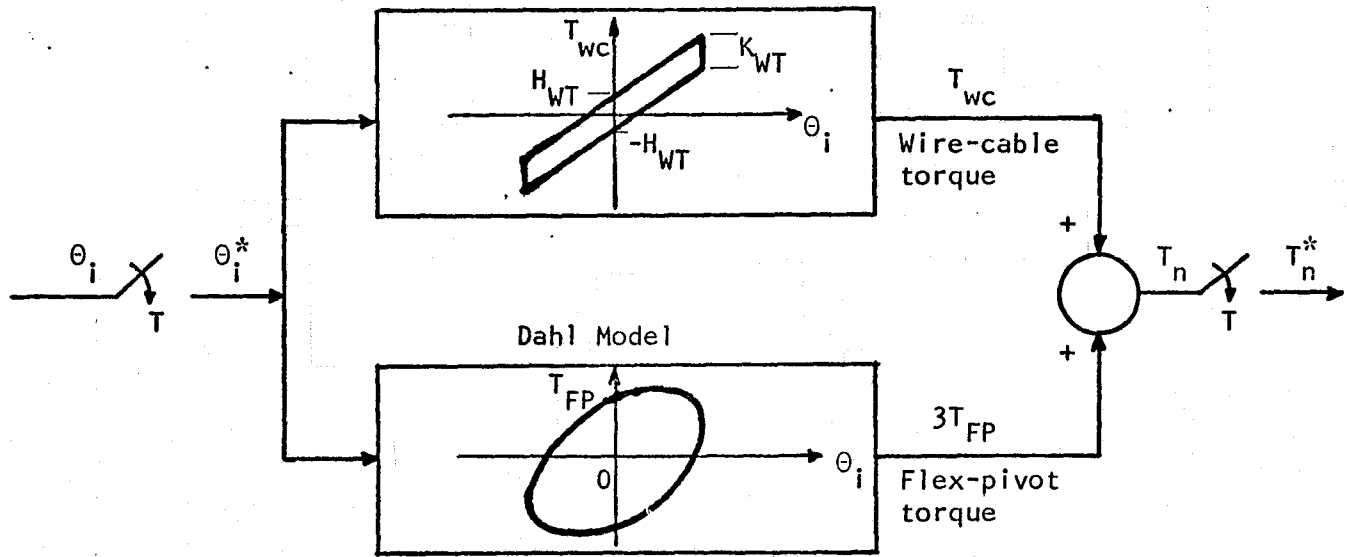


Figure 4-2. Discrete model of the combined nonlinearity of the wire-cable and flex-pivot torques.

$$T_{wc}^-(\theta_i) = -H_{WT} + K_{WT}\theta_i \quad \dot{\theta}_i \leq 0 \quad (4-3)$$

where H_{WT} is in N-m, K_{WT} in N-m/rad. θ_i is in rad, and $T_{wc}(\theta_i)$ in N-m.

It has been established that the Dahl solid rolling friction characteristics can be approximated by the nonlinear relation,

$$\frac{dT_{FP}(\theta_i)}{d\theta_i} = \gamma(T_{FPI} - T_{FP0})^i \quad (4-4)$$

where

i = positive number

γ = positive constant

$$T_{FPI} = T_{FP} \text{SGN}(\dot{\theta}_i)$$

T_{FP0} = saturation level of T_{FP}

For $i = 2$, Eq. (4-4) is integrated to give

$$\theta_i + c_1 = \frac{-1}{\gamma(T_{FP}^+ - T_{FP0})} \quad \dot{\theta}_i \geq 0 \quad (4-5)$$

$$\theta_i + c_2 = \frac{-1}{\gamma(T_{FP}^- + T_{FP0})} \quad \dot{\theta}_i \leq 0 \quad (4-6)$$

where C_1 and C_2 are constants of integration, and

$$T_{FP}^+ = T_{FP} \quad \dot{\theta}_i \geq 0 \quad (4-7)$$

$$T_{FP}^- = T_{FP} \quad \dot{\theta}_i \leq 0 \quad (4-8)$$

The constants of integration are determined at the initial point where

$$\theta_{ii} = \text{initial value of } \theta_i$$

$$T_{FPi} = \text{initial value of } T_{FP}$$

Then,

$$C_1 = -\theta_{ii} - \frac{1}{\gamma(T_{FPi}^+ - T_{FPO})} \quad \dot{\theta}_i \geq 0 \quad (4-9)$$

$$C_2 = -\theta_{ii} - \frac{1}{\gamma(T_{FPi}^- + T_{FPO})} \quad \dot{\theta}_i \leq 0 \quad (4-10)$$

The describing function analysis depends on the assumption that the input to the nonlinearity is a sine wave. Let $\theta_i(t)$ be described by the cosinusoidal function,

$$\theta_i(t) = A \cos \omega t \quad (4-11)$$

$$\dot{\theta}_i(t) = -A \omega \sin \omega t \quad (4-12)$$

$$\text{Thus,} \quad \theta_{ii} = -A \quad \dot{\theta}_i \geq 0 \quad (4-13)$$

$$\theta_{ii} = A \quad \dot{\theta}_i \leq 0 \quad (4-14)$$

The constant of integration in Eqs. (4-9) and (4-10) become

$$C_1 = A - \frac{1}{\gamma(T_{FPi}^+ - T_{FPO})} \quad (4-15)$$

$$C_2 = -A - \frac{1}{\gamma(T_{FPi}^- + T_{FPO})} \quad (4-16)$$

Substitution of Eqs. (4-11) and (4-15) in Eq. (4-5) and simplifying, the solution of T_{FP}^+ is written as

$$T_{FP}^+(t) = T_{FP0} \frac{\frac{R}{R-1} + \frac{a}{2}(1 - \cos\omega t)}{\frac{a}{2}(1 - \cos\omega t) + \frac{1}{R-1}} \quad (4-17)$$

which is valid for $\dot{\theta}_i \geq 0$ or $(2k+1)\pi \leq \omega t \leq 2(k+1)\pi$, $k = 0, 1, 2, \dots$,

where

$$a = 2\gamma AT_{FP0} \quad (4-18)$$

$$R = -\frac{1}{a} + \sqrt{\frac{a^2 + 1}{a^2}} = \frac{T_{FPi}}{T_{FP0}} \quad (4-19)$$

Similarly, for $\dot{\theta}_i \leq 0$, using Eqs. (4-11) and (4-16) in Eq. (4-6), we have

$$T_{FP}^- = T_{FP0} \frac{\frac{R}{R+1} - \frac{a}{2}(1 - \cos\omega t)}{\frac{a}{2}(1 - \cos\omega t) + \frac{1}{R+1}} \quad (4-20)$$

which is valid for $2k\pi \leq \omega t \leq (2k+1)\pi$, $k = 0, 1, 2, \dots$

The relations for T_{FP}^+ and T_{FP}^- in Eqs. (4-17) and (4-20) together with those of $T_{WC}(\theta_i)$ in Eqs. (4-2) and (4-3) are used for the derivation of the discrete describing function of the combined nonlinearity. As shown in Fig. 4-2, the total torque disturbance due to the combined nonlinearity is given

by

$$\begin{aligned} T_n^+ &= T_{WC}^+ + 3T_{FP}^+ \\ &= H_{WT} + K_{WT}A\cos\omega t + 3T_{FP0} \frac{\frac{R}{R-1} + \frac{a}{2}(1 - \cos\omega t)}{\frac{a}{2}(1 - \cos\omega t) + \frac{1}{R-1}} \quad \dot{\theta}_i \geq 0 \end{aligned} \quad (4-21)$$

$$\begin{aligned} T_n^- &= T_{WC}^- + 3T_{FP}^- \\ &= -H_{WT} + K_{WT}A\cos\omega t + 3T_{FP0} \frac{\frac{R}{R+1} - \frac{a}{2}(1 - \cos\omega t)}{\frac{a}{2}(1 - \cos\omega t) + \frac{1}{R+1}} \quad \dot{\theta}_i \leq 0 \end{aligned} \quad (4-22)$$

For the discrete model, we let

$$\theta_i(t) = A\cos(\omega t + \phi) \quad (4-23)$$

where ϕ denotes the phase in radians. The z-transform of $\theta_i(t)$ is

$$\Theta_i(z) = \sum_{k=0}^{\infty} A \cos\left(\frac{2\pi k}{N} + \phi\right) z^{-k} \quad (4-24)$$

$N = 2, 3, \dots$ Or, in closed form,

$$\Theta_i(z) = \frac{Az[(z - \cos 2\pi/N)\cos\phi - \sin 2\pi/N \sin\phi]}{z^2 - 2z\cos 2\pi/N + 1} \quad (4-25)$$

The z-transform of $T_n(t)$ is denoted by $T_n(z)$. Then, the discrete describing function of the combined nonlinearity is defined as

$$N(z) = \frac{T_n(z)}{\Theta_i(z)} \quad (4-26)$$

The discrete describing function (DDF) for $N = 2$ is derived separately in the following section.

4.2 The DDF of the Combined Nonlinearity For $N = 2$

Let $T_n(kT)$ denote the value of $T_n^*(t)$ at $t = kT$. For $N = 2$, the signal $T_n^*(t)$ is a periodic function with a period of $2T$. The z-transform of $T_n^*(t)$ is written as

$$\begin{aligned} T_n(z) &= T_n(0)(1 + z^{-2} + z^{-4} + \dots) + T_n(T)(z^{-1} + z^{-3} + \dots) \\ &= \frac{T_n(0)z^2 + T_n(T)z}{z^2 - 1} \end{aligned} \quad (4-27)$$

For the cosinusoidal input of Eq. (4-23), the corresponding expression for $T_{FP}^+(t)$ and $T_{FP}^-(t)$ are

$$T_{FP}^+(t) = T_{FP0} \frac{\frac{R}{R-1} + \frac{a}{2}(1 - \cos(\omega t + \phi))}{\frac{1}{R-1} + \frac{a}{2}(1 - \cos(\omega t + \phi))} \quad \dot{\Theta}_i \geq 0 \quad (4-28)$$

$$T_{FP}^-(t) = T_{FP0} \frac{\frac{R}{R+1} - \frac{a}{2}(1 - \cos(\omega t + \phi))}{\frac{1}{R+1} + \frac{a}{2}(1 - \cos(\omega t + \phi))} \quad \dot{\Theta}_i \leq 0 \quad (4-29)$$

respectively. For $t = kT$, the last two equations become

$$T_{FP}^+(kT) = T_{FP0} \frac{\frac{R}{R-1} + \frac{a}{2}(1 - \cos(\frac{2\pi k}{N} + \phi))}{\frac{1}{R-1} + \frac{a}{2}(1 - \cos(\frac{2\pi k}{N} + \phi))} \quad \dot{\Theta}_i \geq 0 \quad (4-30)$$

$$T_{FP}^-(kT) = T_{FP0} \frac{\frac{R}{R+1} - \frac{a}{2}(1 - \cos(\frac{2\pi k}{N} + \phi))}{\frac{1}{R+1} + \frac{a}{2}(1 - \cos(\frac{2\pi k}{N} + \phi))} \quad \dot{\Theta}_i \leq 0 \quad (4-31)$$

For $N = 2$, Eq. (4-25) is simplified to

$$\Theta_i(z) = \frac{Az \cos \phi}{z + 1} \quad (4-32)$$

Substitution of Eqs. (4-32) and (4-27) into Eq. (4-26), we have

$$N(z) = \frac{T_n(z)}{\Theta_i(z)} = \frac{T_n(0)z + T_n(T)}{A(z-1)\cos \phi} \quad (4-33)$$

Also, for $N = 2$, $z = -1$; the last equation is simplified to

$$N(z) = \frac{T_n(0) - T_n(T)}{2A \cos \phi} \quad (4-34)$$

For $N = 2$,

$$T_n(0) = T_n^-(0) \quad 0 \leq \phi < \pi \quad (\dot{\Theta}_i \geq 0)$$

$$= T_n^+(0) \quad \pi \leq \phi < 2\pi \quad (\dot{\Theta}_i \leq 0)$$

$$T_n(T) = T_n^+(T) \quad 0 \leq \phi < \pi \quad (\dot{\Theta}_i \geq 0)$$

$$= T_n^-(T) \quad \pi \leq \phi < 2\pi \quad (\dot{\Theta}_i \leq 0)$$

Then, Eq. (4-34) becomes

$$N(z) = \frac{T_n^-(0) - T_n^+(T)}{2A \cos \phi} \quad 0 \leq \phi < \pi \quad (4-35)$$

$$N(z) = \frac{T_n^+(0) - T_n^-(T)}{2A \cos \phi} \quad \pi \leq \phi < 2\pi \quad (4-36)$$

For stability analysis, it is convenient to define

$$F(z) = -\frac{1}{N(z)} \quad (4-37)$$

Using Eqs. (4-2), (4-3), (4-30) and (4-31), we have

$$T_n^+(0) = H_{WT} + K_{WT}A\cos\phi + 3T_{FP0} \frac{\frac{R}{R-1} + \frac{a}{2}(1 - \cos\phi)}{\frac{1}{R-1} + \frac{a}{2}(1 - \cos\phi)} \quad (4-38)$$

$$T_n^-(0) = -H_{WT} + K_{WT}A\cos\phi + 3T_{FP0} \frac{\frac{R}{R+1} - \frac{a}{2}(1 - \cos\phi)}{\frac{1}{R-1} + \frac{a}{2}(1 - \cos\phi)} \quad (4-39)$$

$$\begin{aligned} T_n^+(T) &= H_{WT} + K_{WT}A\cos(\phi + \pi) + 3T_{FP0} \frac{\frac{R}{R-1} + \frac{a}{2}(1 - \cos(\pi + \phi))}{\frac{1}{R-1} + \frac{a}{2}(1 - \cos(\pi + \phi))} \\ &= H_{WT} - K_{WT}A\cos\phi + 3T_{FP0} \frac{\frac{R}{R-1} + \frac{a}{2}(1 + \cos\phi)}{\frac{1}{R-1} + \frac{a}{2}(1 + \cos\phi)} \end{aligned} \quad (4-40)$$

$$T_n^-(T) = -H_{WT} - K_{WT}A\cos\phi + 3T_{FP0} \frac{\frac{R}{R+1} - \frac{a}{2}(1 + \cos\phi)}{\frac{1}{R+1} + \frac{a}{2}(1 + \cos\phi)} \quad (4-41)$$

Thus, for $0 \leq \phi < \pi$,

$$\begin{aligned} T_c^-(0) - T_c^+(T) &= 2K_{WT}A\cos\phi - 2H_{WT} + 3T_{FP0} \left[\frac{\frac{R}{R+1} - \frac{a}{2}(1 - \cos\phi)}{\frac{1}{R+1} + \frac{a}{2}(1 - \cos\phi)} \right. \\ &\quad \left. - \frac{\frac{R}{R-1} + \frac{a}{2}(1 + \cos\phi)}{\frac{1}{R+1} + \frac{a}{2}(1 - \cos\phi)} \right] \end{aligned} \quad (4-42)$$

For $\pi \leq \phi < 2\pi$,

$$\begin{aligned} T_c^+(0) - T_c^-(T) &= 2K_{WT}A\cos\phi + 2H_{WT} + 3T_{FP0} \left[\frac{\frac{R}{R-1} + \frac{a}{2}(1 - \cos\phi)}{\frac{1}{R-1} + \frac{a}{2}(1 - \cos\phi)} \right. \\ &\quad \left. - \frac{\frac{R}{R+1} - \frac{a}{2}(1 + \cos\phi)}{\frac{1}{R+1} + \frac{a}{2}(1 + \cos\phi)} \right] \end{aligned} \quad (4-43)$$

4.3 Properties of $F(z) = -1/N(z)$ for $N = 2$ as $A \rightarrow 0$ and $A \rightarrow \infty$

The properties of $F(z)$ for $N = 2$ as $A \rightarrow 0$ and $A \rightarrow \infty$ are now investigated. These properties will be useful in the determination of the critical regions of $F(z)$ for stability studies.

Theorem 4-1.

For $N = 2$,

$$\lim_{A \rightarrow \infty} F(z) = \lim_{A \rightarrow \infty} -1/N(z) = -1/K_{WT} \quad \text{for all } \phi \quad (4-44)$$

Proof: From Eq. (4-19),

$$\frac{R}{R-1} = \frac{-1 + \sqrt{a^2 + 1}}{-1 - a + \sqrt{a^2 + 1}} \quad (4-45)$$

$$\frac{R}{R+1} = \frac{-1 + \sqrt{a^2 + 1}}{-1 + a + \sqrt{a^2 + 1}} \quad (4-46)$$

$$\frac{1}{R-1} = \frac{a}{-1 - a + \sqrt{a^2 + 1}} \quad (4-47)$$

$$\frac{1}{R+1} = \frac{a}{-1 + a + \sqrt{a^2 + 1}} \quad (4-48)$$

and $a = 2\gamma A T_{FP0}$.

Let $F^+(z) = F(z)$ for $0 \leq \phi < \pi$. Substituting Eq. (4-35) into Eq. (4-37), we have

$$F^+(z) = \frac{-2A \cos \phi}{T_n^-(0) - T_n^+(T)} \quad (4-49)$$

Then,

$$\lim_{A \rightarrow \infty} F^+(z) = \lim_{A \rightarrow \infty} \frac{-2A \cos \phi}{T_n^-(0) - T_n^+(T)} \quad (4-50)$$

Substituting Eqs. (4-39) and (4-40) into the last equation and using Eqs. (4-45) through (4-48), we get

$$\lim_{A \rightarrow \infty} F^+(z) =$$

$$\lim_{A \rightarrow \infty} \frac{-2A \cos \phi}{3T_{FPO} \left[\frac{\frac{-1 + \sqrt{a^2 + 1}}{-1 + a + \sqrt{a^2 + 1}} - \frac{a}{2}(1 - \cos \phi)}{\frac{a}{-1 + a + \sqrt{a^2 + 1}} + \frac{a}{2}(1 - \cos \phi)} - \frac{\frac{-1 + \sqrt{a^2 + 1}}{-1 - a + \sqrt{a^2 + 1}} + \frac{a}{2}(1 + \cos \phi)}{\frac{a}{-1 - a + \sqrt{a^2 + 1}} + \frac{a}{2}(1 + \cos \phi)} \right] + \frac{2K_{WT} A \cos \phi - 2H_{WT}}{}}$$

$$= \lim_{A \rightarrow \infty} \frac{-2A \cos \phi}{3T_{FPO} \left[\frac{\frac{1}{2} - \frac{a}{2}(1 - \cos \phi)}{\frac{1}{2} + \frac{a}{2}(1 - \cos \phi)} - \frac{-a + \frac{a}{2}(1 + \cos \phi)}{-a + \frac{a}{2}(1 + \cos \phi)} \right] + \frac{2K_{WT} A \cos \phi - 2H_{WT}}{}}$$

$$= \lim_{A \rightarrow \infty} \frac{-2A \cos \phi}{-6T_{FPO} + 2K_{WT} A \cos \phi - 2H_{WT}} = \lim_{A \rightarrow \infty} \frac{-A \cos \phi}{K_{WT} A \cos \phi} = -\frac{1}{K_{WT}} \quad \text{Q.E.D.}$$

Similarly, for $\pi \leq \phi < 2\pi$, $F^-(z) = F(z)$,

$$\lim_{A \rightarrow \infty} F^-(z) = \lim_{A \rightarrow \infty} \frac{-2A \cos \phi}{T_n^+(0) - T_n^-(T)}$$

$$= \lim_{A \rightarrow \infty} \frac{-2A \cos \phi}{3T_{FPO} \left[\frac{\frac{-1 + \sqrt{a^2 + 1}}{-1 - a + \sqrt{a^2 + 1}} + \frac{a}{2}(1 - \cos \phi)}{\frac{a}{-1 + a + \sqrt{a^2 + 1}} - \frac{a}{2}(1 - \cos \phi)} - \frac{\frac{-1 + \sqrt{a^2 + 1}}{-1 + a + \sqrt{a^2 + 1}} - \frac{a}{2}(1 + \cos \phi)}{\frac{a}{-1 + a + \sqrt{a^2 + 1}} + \frac{a}{2}(1 + \cos \phi)} \right] + \frac{2K_{WT} A \cos \phi + 2H_{WT}}{}}$$

$$= \lim_{A \rightarrow \infty} \frac{-2A \cos \phi}{3T_{FPO} \left[\frac{-a + \frac{a}{2}(1 - \cos \phi)}{\frac{1}{2} + \frac{a}{2}(1 - \cos \phi)} - \frac{\frac{1}{2} - \frac{a}{2}(1 - \cos \phi)}{\frac{1}{2} + \frac{a}{2}(1 + \cos \phi)} \right] + \frac{2K_{WT} A \cos \phi + 2H_{WT}}{}}$$

$$= \lim_{A \rightarrow \infty} \frac{-2A \cos \phi}{6T_{FPO} + 2K_{WT} A \cos \phi + 2H_{WT}} = -\frac{1}{K_{WT}} \quad \text{Q.E.D.}$$

Theorem 4-2.

For $N = 2$,

$$\lim_{A \rightarrow 0} F(z) = \lim_{A \rightarrow 0} -\frac{1}{N(z)} = \underline{0/180^\circ + \tan^{-1} \frac{\cos \phi}{|\cos \phi|}} \quad \text{for all } \phi \quad (4-51)$$

Proof: For $0 \leq \phi < \pi$,

$$\lim_{A \rightarrow 0} F^+(z) =$$

$$\begin{aligned} & \lim_{A \rightarrow 0} \frac{-2A \cos \phi}{3T_{FP0} \left[\frac{-1 + \sqrt{a^2 + 1}}{-1 + a + \sqrt{a^2 + 1}} - \frac{a}{2}(1 - \cos \phi) - \frac{-1 + \sqrt{a^2 + 1}}{-1 - a + \sqrt{a^2 + 1}} + \frac{a}{2}(1 + \cos \phi) \right] + \frac{a}{-1 + a + \sqrt{a^2 + 1}} + \frac{a}{2}(1 - \cos \phi) - \frac{a}{-1 - a + \sqrt{a^2 + 1}} + \frac{a}{2}(1 + \cos \phi)} \\ & \quad + \overline{2K_{WT} A \cos \phi - 2H_{WT}} \\ & = \lim_{A \rightarrow 0} \frac{-2A \cos \phi}{3T_{FP0} \left[\frac{\frac{a}{1+a} - \frac{a}{2}(1 - \cos \phi)}{\frac{1}{1+a} + \frac{a}{2}(1 - \cos \phi)} - \frac{\frac{a}{-1+a} + \frac{a}{2}(1 + \cos \phi)}{\frac{1}{-1+a} + \frac{a}{2}(1 + \cos \phi)} \right] + \overline{2K_{WT} A \cos \phi - 2H_{WT}}} \\ & = \lim_{A \rightarrow 0} \frac{-2A \cos \phi}{-2H_{WT}} = \underline{0/0^\circ} \quad \text{for } 0 \leq \phi < \pi/2 \\ & \quad = \underline{0/180^\circ} \quad \text{for } \pi/2 < \phi \leq \pi \end{aligned}$$

Similarly, for $\pi \leq \phi < 2\pi$,

$$\lim_{A \rightarrow 0} F^-(z) =$$

$$\begin{aligned} & \lim_{A \rightarrow 0} \frac{-2A \cos \phi}{3T_{FP0} \left[\frac{-1 + \sqrt{a^2 + 1}}{-1 - a + \sqrt{a^2 + 1}} + \frac{a}{2}(1 - \cos \phi) - \frac{-1 + \sqrt{a^2 + 1}}{-1 + a + \sqrt{a^2 + 1}} - \frac{a}{2}(1 + \cos \phi) \right] + \frac{a}{-1 + a + \sqrt{a^2 + 1}} + \frac{a}{2}(1 - \cos \phi) - \frac{a}{-1 - a + \sqrt{a^2 + 1}} + \frac{a}{2}(1 + \cos \phi)} \\ & \quad + \overline{2K_{WT} A \cos \phi + 2H_{WT}} \end{aligned}$$

$$\begin{aligned}
\lim_{A \rightarrow 0} F^-(z) &= \lim_{A \rightarrow 0} \frac{-2A \cos \phi}{3T_{FP0} \left[\frac{\frac{a}{-1+a} + \frac{a}{2}(1 - \cos \phi)}{\frac{1}{1+a} + \frac{a}{2}(1 - \cos \phi)} - \frac{\frac{a}{1+a} - \frac{a}{2}(1 + \cos \phi)}{\frac{1}{1+a} + \frac{a}{2}(1 + \cos \phi)} \right] + 2K_{WT} A \cos \phi + 2H_{WT}} \\
&= \lim_{A \rightarrow 0} \frac{-2A \cos \phi}{2K_{WT} A \cos \phi + 2H_{WT}} \\
&= \frac{0/180^\circ + \tan^{-1} \frac{\cos \phi}{\cos \phi}}{0/0^\circ} = \frac{0/180^\circ}{0/0^\circ} \quad \begin{matrix} 3\pi/2 \leq \phi < 2\pi \\ \pi \leq \phi < 3\pi/2 \end{matrix} \quad \text{Q.E.D.}
\end{aligned}$$

4.4 The DDF of the Combined Nonlinearity For $N \geq 3$

A general relation can be derived for the combined nonlinearity for $N \geq 3$.

In general, the z-transform of the output of the combined nonlinearity may be written as

$$\begin{aligned}
T_q(z) &= \sum_{m=0}^{\infty} \sum_{k=0}^{N-1} T_n(kT) z^{-k-mN} \\
&= \frac{\sum_{k=0}^{N-1} T_n(kT) z^{N-k}}{z^N - 1} \quad (4-52)
\end{aligned}$$

The discrete describing function then becomes

$$N(z) = \frac{T_n(z)}{\theta_i(z)} = \frac{\sum_{k=0}^{N-1} T_n(kT) z^{N-k}}{(z^N - 1) \sum_{k=0}^{\infty} (A \cos \frac{2\pi k}{N} + \phi) z^{-k}} \quad (4-53)$$

The last equation is simplified to

$$N(z) = \frac{\sum_{k=0}^{N-1} T_n(kT) z^{N-k-1}}{A \sum_{k=0}^{N-1} (\cos \frac{2\pi k}{N} + \phi) z^{N-k-1}} \quad (N \geq 3) \quad (4-54)$$

Or, alternately,

$$N(z) = \frac{\sum_{k=0}^{N-1} T_n(kT) z^{N-k} (z^2 - 2z \cos \frac{2\pi}{N} + 1)}{\sum_{k=0}^{N-1} (z - e^{j2\pi k/N}) A z ((z - \cos \frac{2\pi}{N}) \cos \phi - \sin \frac{2\pi}{N} \sin \phi)} \quad (4-55)$$

Or,

$$N(z) = \frac{\sum_{k=0}^{N-1} T_n(kT) z^{N-k-1}}{A(z-1) \sum_{k=2}^{N-2} (z - e^{j2\pi k/N}) ((z - \cos \frac{2\pi}{N}) \cos \phi - \sin \frac{2\pi}{N} \sin \phi)} \quad (4-56)$$

For $N = 3$, $z = e^{j2\pi/3}$,

$$N(z) = \frac{T_n(0)z^2 + T_n(T)z + T_n(2T)}{A(z-1)((z+0.5)\cos\phi - 0.866\sin\phi)} \quad (4-57)$$

Similar expressions can be obtained for $N = 4, 5, \dots$ with z identified with $e^{j2\pi/N}$.

In general,

$$\begin{aligned} T_n(kT) &= T_n^-(kT) & 0 < \frac{2\pi k}{N} + \phi < \pi \\ &= T_n^+(kT) & \pi < \frac{2\pi k}{N} + \phi < 2\pi \end{aligned} \quad (4-58)$$

4.5 Asymptotic Properties of $-1/N(z)$ for $N \geq 3$ as A Approaches Infinity

The following properties of $-1/N(z)$ are found for $N \geq 3$. The proofs of these properties can be obtained the same way as those for $N = 2$ by replacing ϕ by $\phi + 2\pi k/N$.

$$(a) \lim_{A \rightarrow \infty} \{-1/N(z)\} = -\frac{1}{K_{WT}} \quad \text{for all } \phi \quad (4-59)$$

$$(b) \lim_{A \rightarrow \infty} |-1/N(z)| = \frac{1}{K_{WT}} \quad \text{for all } \phi \quad (4-60)$$

$$(c) \lim_{A \rightarrow \infty} \{\text{Arg}(-1/N(z))\} = 180^\circ \quad \text{for all } \phi \quad (4-61)$$

4.6 Asymptotic Properties of $-1/N(z)$ for $N \geq 3$ as A Approaches Zero

The following properties of $-1/N(z)$ for $N \geq 3$ are obtained as A

approaches zero.

(a) For $N \geq 3$, and for all ϕ ,

$$\lim_{A \rightarrow 0} |1/N(z)| = 0 \quad (4-62)$$

(b) For $N \geq 3$, (N = odd integers)

$$\lim_{A \rightarrow 0} \text{Arg}(-1/N(z)) = - \left(\frac{1 + 3N + 2k}{2N} \right) \pi + \phi \quad (4-63)$$

for $k\pi/N \leq \phi < (k+1)\pi/N$, $k = 0, 1, 2, \dots, (2N-1)$.

(c) For $N \geq 4$, (N = even integers)

$$\lim_{A \rightarrow 0} \text{Arg}(-1/N(z)) = - \left(\frac{2 + 3N + 4k}{2N} \right) \pi + \phi \quad (4-64)$$

for $2k\pi/N \leq \phi < 2(k+1)\pi/N$.

In view of the properties of $-1/N(z)$ listed above, the following theorems are generated.

Theorem 4-3.

For even integral $N \geq 3$, the magnitude and phase of $-1/N(z)$ repeat for every $\phi = 2\pi/N$ radians.

Theorem 4-4.

For odd N ($N \geq 3$), the magnitude and phase of $-1/N(z)$ repeat for every $= \pi/N$ radians.

4.7 Discrete Describing Function Plots of the Combined Wire-Cable and Flex-Pivot Nonlinearity - The Critical Regions

The discrete describing function, $N(z)$, for the combined wire-cable and flex-pivot nonlinearity is derived in the preceding sections. The plots of $F(z) = -1/N(z)$ together with the plot of $G_{eq}(z)$, which is the linear transfer function that $N(z)$ sees, in the frequency domain allow the study of the condition of self-sustained oscillations of the digital IPS system.

Computer programs for the evaluation of the $-1/N(z)$ for $N = 2$ and $N \geq 3$ have been prepared. The listings of these programs are given in Tables 4-1 and 4-2, respectively.

For $N = 2$, the expression for $F(z) = -1/N(z)$ is given in Eqs. (4-35), (4-36) and (4-37). Figure 4-3 shows the $F(z)$ plot for $N = 2$ in the gain-phase coordinates with $0 \leq A < \infty$ and all values of ϕ .

The following set of parameters are used for the nonlinear elements:

$$T_{FP0} = 0.00225$$

$$\gamma = 9.2444 \times 10^4$$

$$K_{WT} = 100$$

$$H_{WT} = 1$$

In view of Theorem 4-1, Eq. (4-44), the most important parameter among those listed above is K_{WT} , since when A approaches infinity the magnitude of $F(z)$ approaches $1/K_{WT}$. However, as shown in Fig. 4-3, the $F(z)$ plot stays on the -180° and -360° axes for $N = 2$.

The discrete describing function $N(z)$ for $N \geq 3$ is given by Eq. (4-54) or Eq. (4-56). Figure 4-4 shows the gain-phase plot of $F(z) = -1/N(z)$ for $N = 3$. The curves for several values of ϕ between 0° and 60° are plotted to illustrate the effect of varying the phase of the input signal to the nonlinearity. It should be noted that for $N = 3$, Theorem 4-3 states that the values of $F(z)$ repeat every 60 degrees starting from $\phi = 0^\circ$. As the magnitude of the input signal, A , approaches infinity, the magnitude of $F(z)$ becomes $1/K_{WT}$ which is -40 db in this case, since K_{WT} is 100. On the other hand, as A approaches zero, the magnitude of $F(z)$ becomes zero or $-\infty$ db, and the phase of $F(z)$ is bounded by -300° and -240° for all values of ϕ . When the value of K_{WT} is varied, the curves of $F(z)$ will shift up or down according to

Table 4-1. Computer program for the computation of the discrete describing function of the combine flex-pivot and wire-cable nonlinearity of the IPS. $N = 2$.

C	CALCULATION FOR $-1/N(Z)$ FOR COMBINED NONLINEARITY, $N=2$
	COMPLEX GN1,GN2
	REAL*8 P(20),RAD,TO,GAMMA,ASTART,A,AA,R,CSS,CSP,CSC
	REAL*8 AA2,R1,R2,R3,R4,TOF,TOM,TTM,TTF,T1,T2
	PI=3.14159D0
	RAD=180.D0/PI
	CSP=1.D0
	TO=0.00225D0
	KWT=100.D0
	HWT=1.D0
	GAMMA=9.2444D4
	ASTART=1.0D-10
	NP=5
	ND=15
	WRITE(5,100)
	WRITE(5,101)
	DO 1 J=1,ND
	DO 1 I=1,NP
	CSS=1.D0-CSP
	CSC=1.D0+CSP
	A=ASTART*DFLOAT(I)*(10.D0**(J-1))
	AA=2.D0*GAMMA*A*TO
	R=(-1.D0/AA)+DSQRT((AA*AA+1.D0)/(AA*AA))
	AA2=AA/2.D0
	R1=1.D0/(R-1.D0)
	R2=R*R1
	R3=1.D0/(R+1.D0)
	R4=R*R3
	TOP=(R2+AA2*CSS)/(R1+AA2*CSS)
	TOM=(R4-AA2*CSS)/(R3+AA2*CSS)
	TTM=(R4-AA2*CSC)/(R3+AA2*CSC)
	TTF=(R2+AA2*CSC)/(R1+AA2*CSC)
	T1=3.D0*TO*(TOF-TTM)+2.D0*(HWT+KWT*AA*CSP)
	T2=3.D0*TO*(TOM-TTF)+2.D0*(HWT+KWT*AA*CSP)
	GN1=-2.D0*AA*CSP/T1
	GN2=-2.D0*AA*CSP/T2
	G11=REAL(GN1)
	G12=AIMAG(GN1)
	G21=REAL(GN2)
	G22=AIMAG(GN2)
	GMAG1=CABS(GN1)
	GMAG2=CABS(GN2)
	GDB1=20.*ALOG10(GMAG1)
	GDB2=20.*ALOG10(GMAG2)
	GPH1=RAD*ATAN2(G12,G11)
	GPH2=RAD*ATAN2(G22,G21)
	IF(GPH2.GE.0.)GPH2=GPH2-360.
	IF(GPH1.GE.0.)GPH1=GPH1-360.
	WRITE(5,102)A,GDB2,GMAG2,GPH2
1	CONTINUE
100	FORMAT(' DISCRETE DESCRIBING FUNCTION FOR IPS ')
101	FORMAT(/,8X,'A',11X,'GDB2',10X,'GMAG',9X,'PHASE'/)
102	FORMAT (1F4E14.5)
	STOP
	END

REPRODUCED
ORIGINAL PAGE

Table 4-2. Computer program for the computation of the discrete describing function of the combined flex-pivot and wire-cable nonlinearity of the IPS. N GE. 3.

```

C      DISCRETE DESCRIBING FUNCTION FOR COMBINED NONLINEARITY, N.GE.3
      REAL PHI,P(15),PI,RAD,GAMMA,ASTART,A,AA,R,HWT,KWT,TD
      REAL PP,RR,AA,R1,R2,R3,R4,AA2,TC,PHIK,PHID,PIK,TWN,TWP
      COMPLEX GV,TTSUM
      COMPLEX TSUMN,ZSUMN,ZSUM,TZ,TSUM,Z,THETA,GMN,GN
      PI=3.14159
      RAD=180./PI
      HWT=1.0
      KWT=100.
      GAMMA=9.2444E4
      ASTART=1.E-8
      ND=9
      NP=1
      TD=0.00225
      RR=0.
      NI=50
      AN=FLOAT(NI)
      N1=NI-1
      N2=NI-2
      P(1)=1.0
      NPFI=3600
      PP=2.*PI/FLOAT(NI)
      THETA=CMPLX(RR,PP)
      Z=CEXP(THETA)
      ZSUMN=CMPLX(1.,0.0)
      TSUMN=CMPLX(0.0,0.0)
      WRITE(5,100)
      WRITE(5,102) AN
      WRITE(5,110) GAMMA
      WRITE(5,111) HWT
      WRITE(5,112) KWT
      WRITE(5,113) TD
      WRITE(5,101)
      DO 8 I=0,144,36
      PHI=(2.0*PI+FLOAT(I))/FLOAT(NPFI)
      PHID=PHI+RAD
      WRITE(5,103)PHID
      DO 1 J=1,ND
      DO 9 L=1,NP
      ZSUMN=CMPLX(1.0,0.0)
      TSUMN=CMPLX(0.0,0.0)
      A=ASTART+FLOAT(L)*(10.**(J-1))
      AA=2.0+GAMMA*A+TD
      AA2=AA/2.0

```

REPRODUCIBILITY OF
ORIGINAL PAGE IS NOT

```

R=(-1.0/AA)+SQRT((AA*AA+1.0)/(AA*AA))
R1=1.0/(R-1.0)
R2=R*R1
R3=1.0/(R+1.0)
R4=R*R3
DO 2 K=0,N1
PIK=(2.0*PI*FLOAT(K))/(FLOAT(N1))
PHIK=PHI+PIK
IF(PHIK.GT.(2.0*PI))PHIK=PHIK-2.0*PI
TWN=-HWT+KWT+A*COS(PHIK)
TWP=HWT+KWT+A*COS(PHIK)
IF(PHIK.LT.PI)GO TO 6
TC=3.0*TD*(R2+AA2-AA2*COS(PHIK))/(R1+AA2-AA2*COS(PHIK))+TWP
GO TO 7
6 TC=3.0*TD*(R4+AA2-AA2*COS(PHIK))/(R3+AA2-AA2*COS(PHIK))+TWN
7 TSUM=TC+Z*(N1-K)
TSUMN=TSUMN+TSUM
2 CONTINUE
IF(N1.LE.3)GO TO 10
DO 3 M=2,N2
ZSUM=Z-Z**M
ZSUMN=ZSUMN+ZSUM
3 CONTINUE
10 CONTINUE
TZ=(Z-COS(P))*COS(PHI)-SIN(P)*SIN(PHI)
GN=TSUMN/(A+TZ*(Z-1.)+ZSUMN)
GNN=-1./GN
GV=GNN
G1=REAL(GV)
G2=AIMAG(GV)
GMAG=CABS(GV)
GDB=20.*ALOG10(GMAG)
GPHASE=RAD*ATAN2(G2,G1)
IF(GPHASE.GE.0.)GPHASE=GPHASE-360.
WRITE(5,104)A,GPHASE,GDB,GMAG
105 FORMAT(1PE24.15)
9 CONTINUE
1 CONTINUE
8 CONTINUE
100 FORMAT(7X,'DESCRIBING FUNCTION OF COMBINED NONLINEARITY')
101 FORMAT(/,7X,'A',10X,'PHASE',10X,'DB',10X,'MAGNITUDE')
102 FORMAT(5X,'N=',F4.1)
110 FORMAT(/,5X,'GAMMA=',1PE12.4)
111 FORMAT(5X,'HWT=',F8.2)
112 FORMAT(5X,'KWT=',F8.2)
113 FORMAT(5X,'TD=',1PE12.2)
103 FORMAT(/,5X,'PHI=',F5.1)
104 FORMAT(1P5E14.5)
STOP
END

```

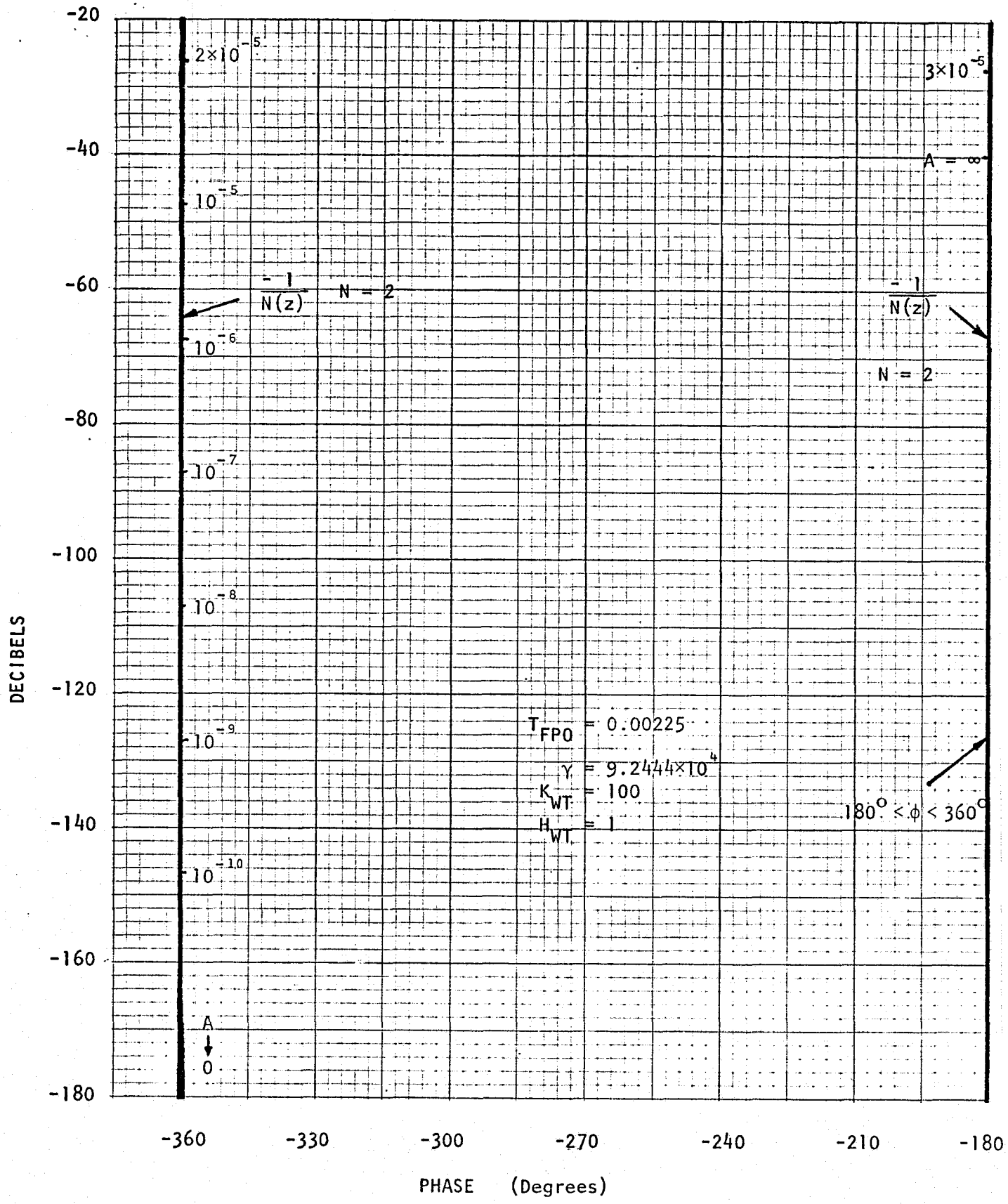
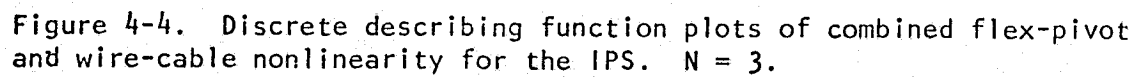


Figure 4-3. Discrete describing function plots of combined flex-pivot and wire-cable nonlinearity for the IPS. $N = 2$.



$1/K_{WT}$ in db; when the values of T_{FP0} , γ , and H_{WT} are varied, the shape of the curved portions of the plots in Fig. 4-4 will be changed. However, in general, the impact of the variation of K_{WT} will be the greatest.

The $F(z)$ plots for $N = 4, 5, 6, 8, 10, 20$, and 50 are shown in Figs. 4-5 through 4-11, respectively. For $N = 4$, the $F(z)$ plot extends from -315° to -225° as ϕ varies. For $N = 5$, the span of the plot is -288° to -252° .

For stability analysis, it is sufficient to consider only the bounds of the $F(z)$ plot for a fixed N . Self-sustained oscillations characterized by the period $T_c = NT$, where T is the sampling period, may occur if $G_{eq}(z)$ intersects with any part of the $F(z)$ plot. The region bounded by all the $F(z)$ curves for a given N is defined as the critical region. The critical regions for the combined nonlinearity for $N > 2$ are the regions that are bounded by the $F(z)$ curves for $\phi = 0^\circ$ and $\phi = 2\pi/N$ for $N = \text{even}$ and $\phi = \pi/N$ for $N = \text{odd}$.

As N approaches infinity, the discrete describing function $N(z)$ approaches the describing function N of the continuous-data nonlinearity, as shown in Fig. 4-11. It is observed that as N increases the width of the critical region becomes narrower. As N approaches infinity, the critical region of $F(z) = -1/N(z)$ approaches the $-1/N$ plot shown in Fig. 2-1.

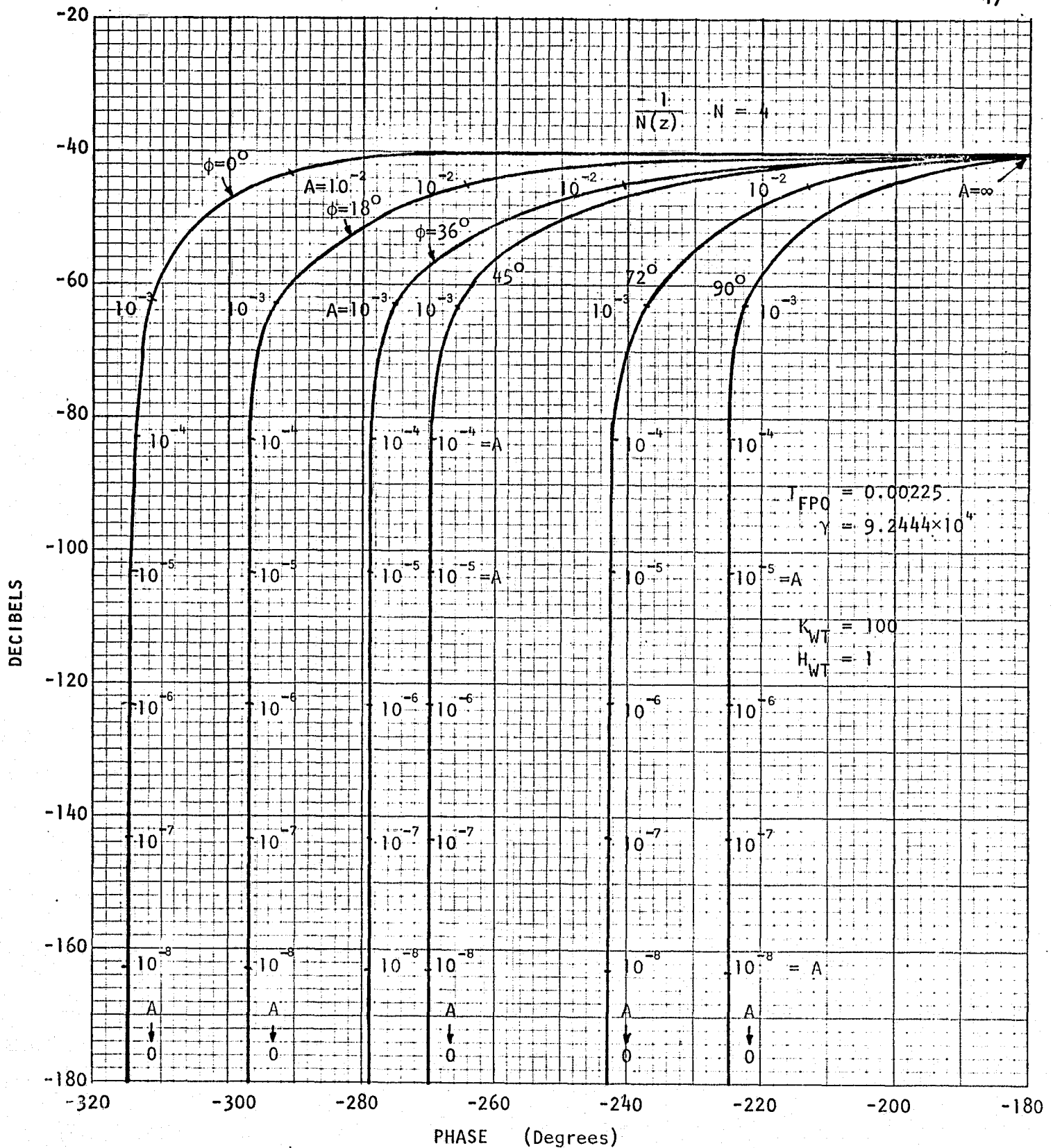


Figure 4-5. Discrete Describing function plots of combined flex-pivot and wire-cable nonlinearity for the IPS. $N = 4$.

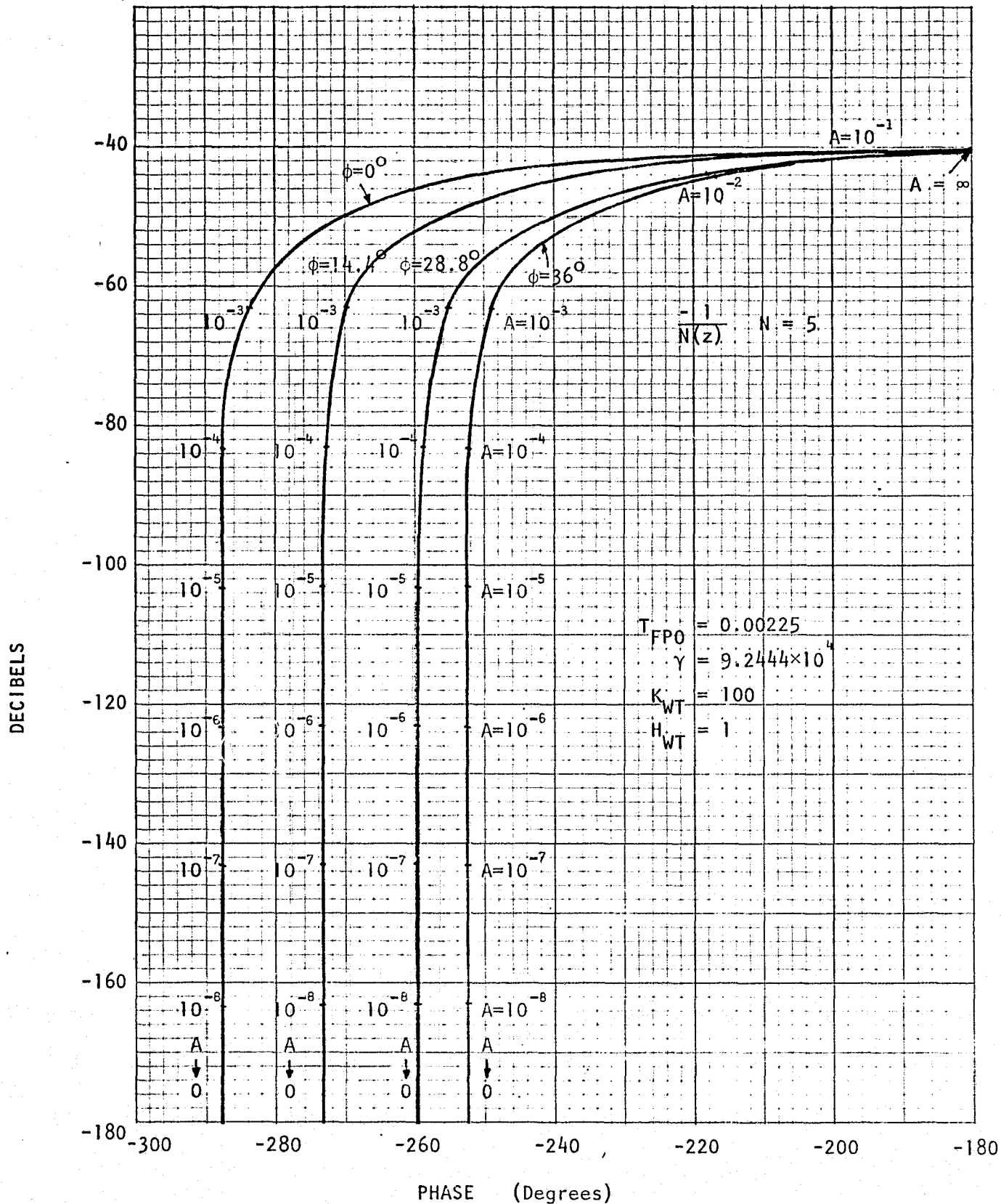


Figure 4-6. Discrete describing function plots of combined flex-pivot and wire-cable nonlinearity for the IPS. $N = 5$.

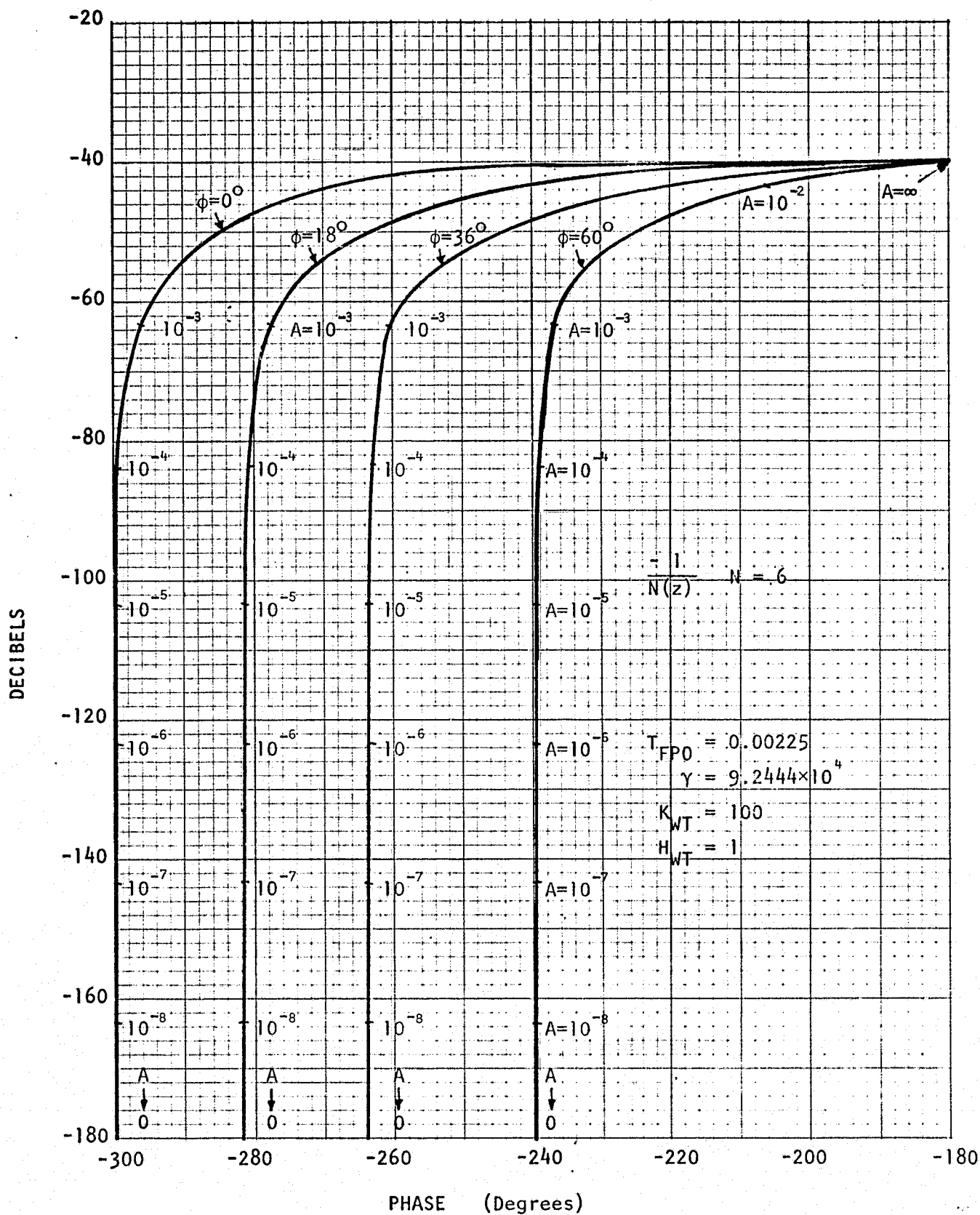


Figure 4-7. Discrete describing function plots of combined flex-pivot and wire-cable nonlinearity for the IPS. $N = 6$.

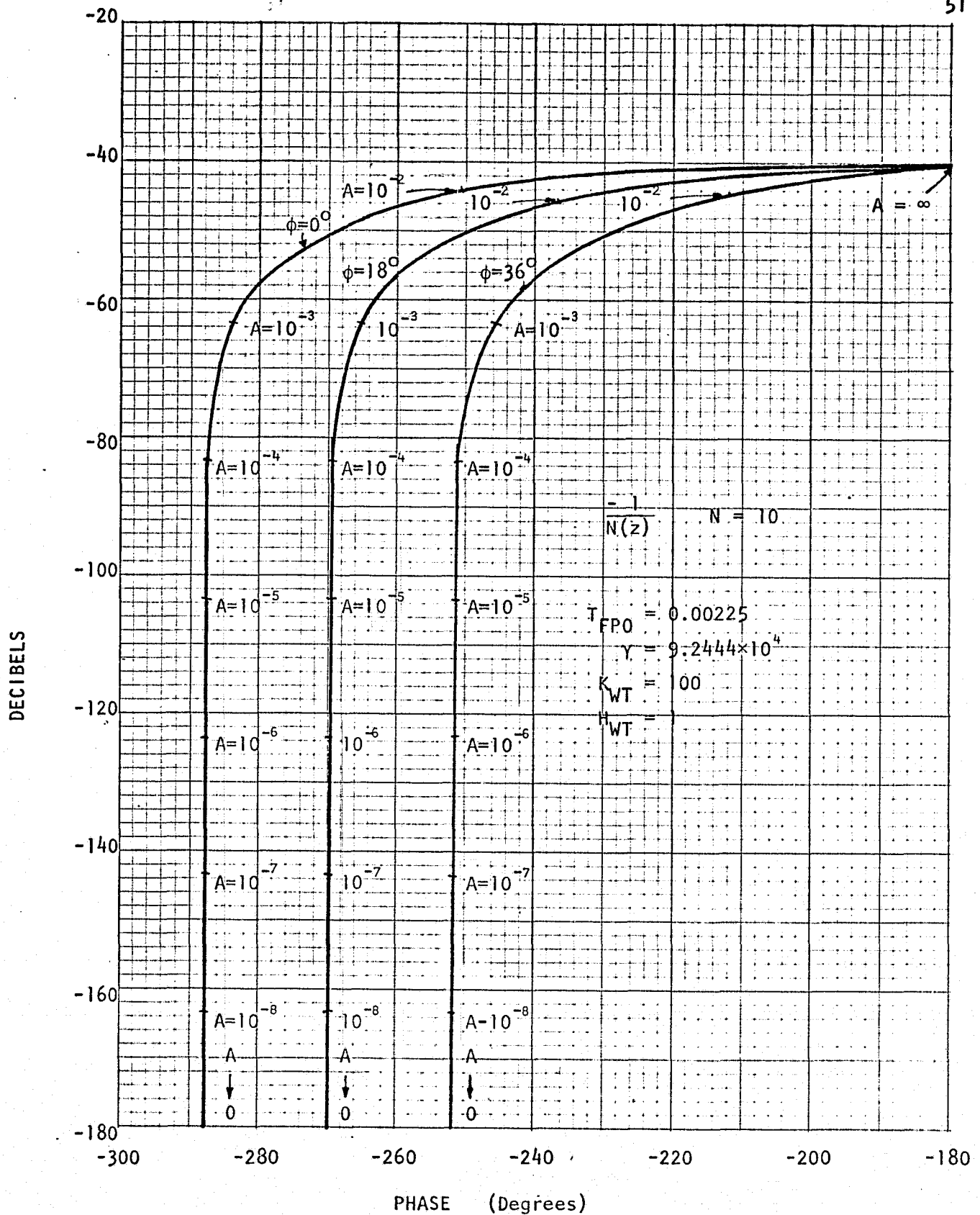


Figure 4-9. Discrete describing function plots of combined flex-pivot and wire-cable nonlinearity for the IPS. $N = 10$.

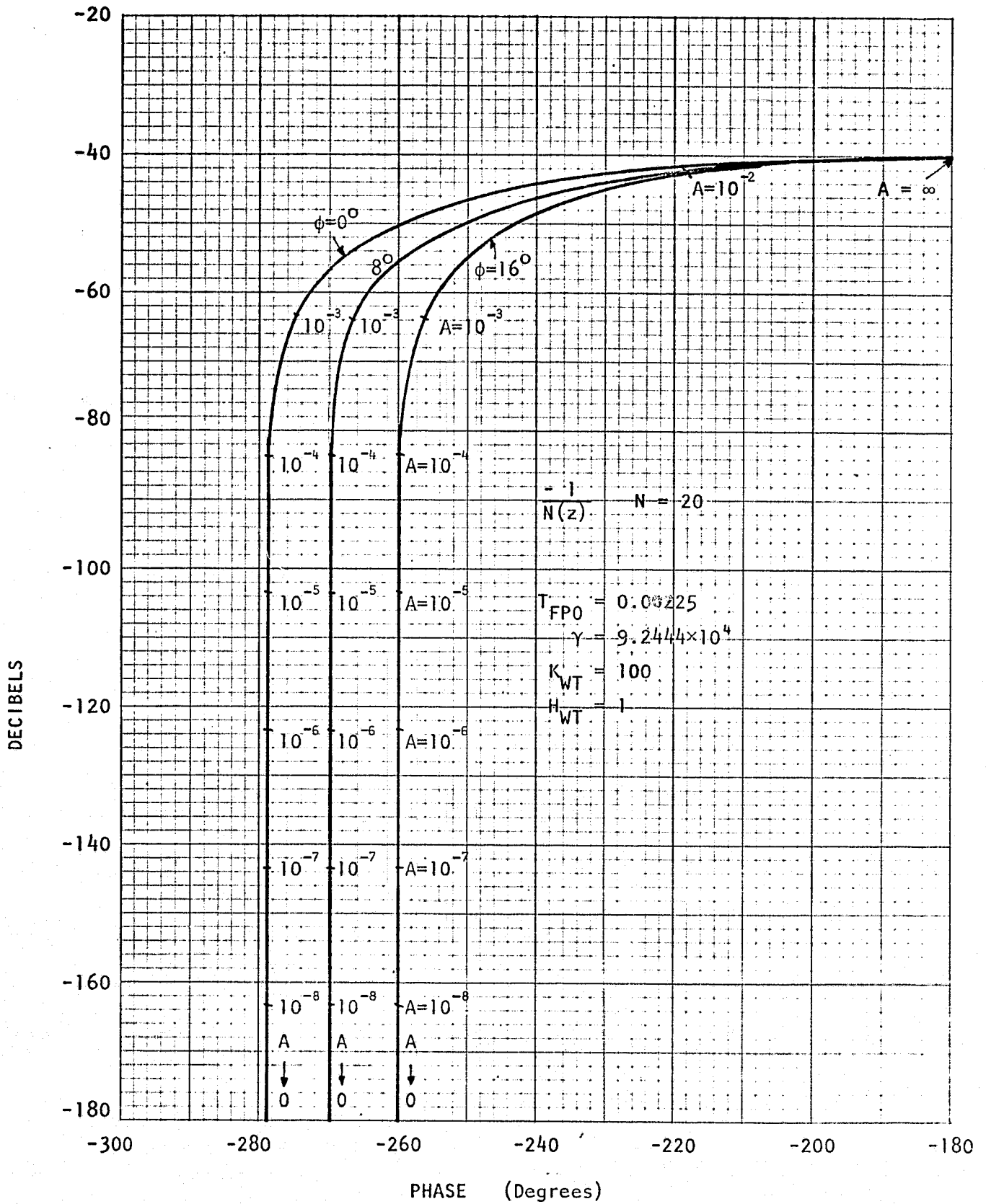


Figure 4-10. Discrete describing function plots of combined flex-pivot and wire-cable nonlinearity for the IPS. $N = 20$.

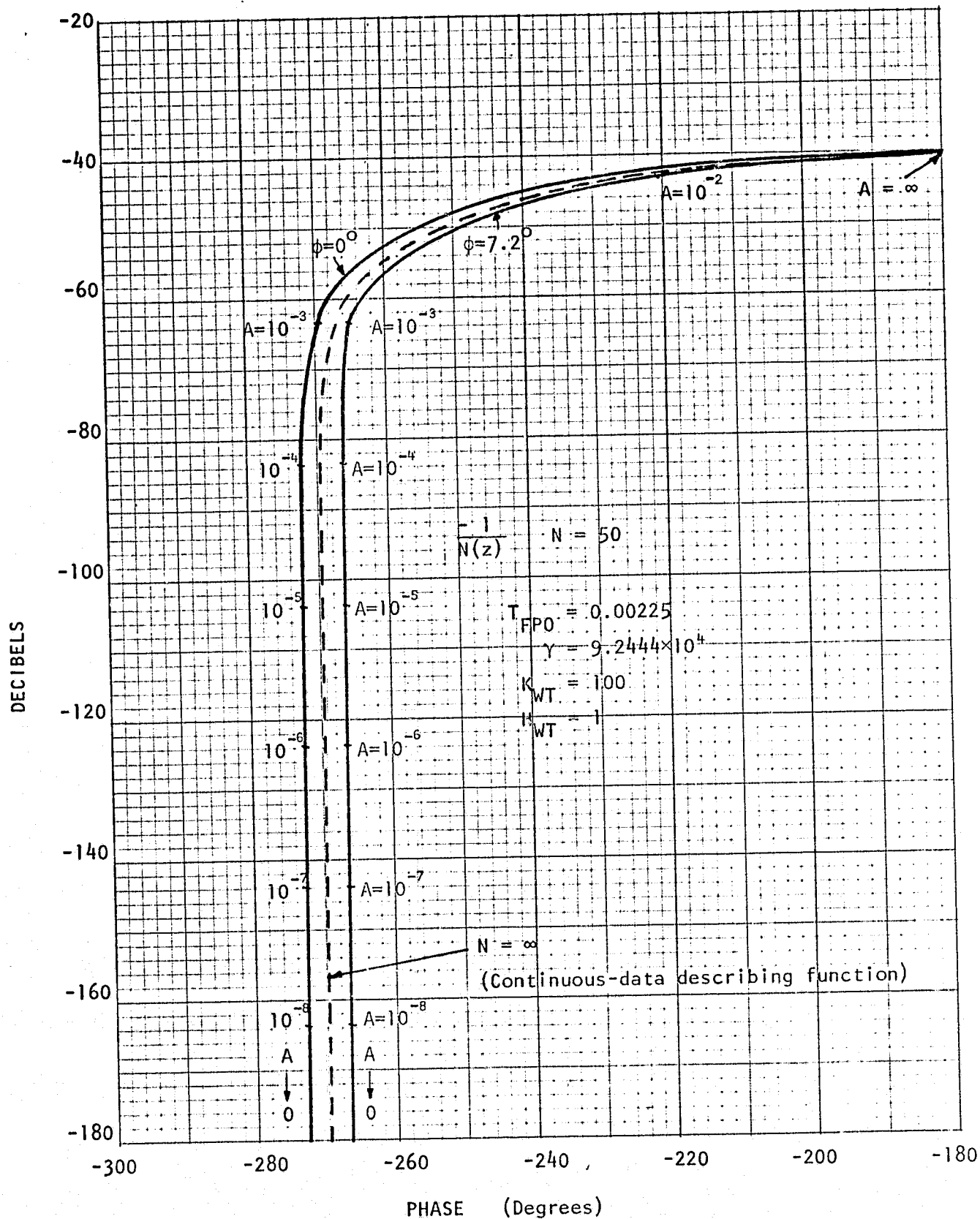


Figure 4-11. Discrete describing function plots of combined flex-pivot and wire-cable nonlinearity for the IPS. $N = 50$.

REFERENCES

1. Final Report, Research Study on IPS Digital Controller Design, V-76,
Systems Research Laboratory, September 1, 1976.